KTH Computer Science
and Communication

Topographical micro-changes in corrugated board production

Effects on flexographic post-print quality

Marcus Rehberger

Licentiate Thesis 2007

Royal Institute of Technology
School of Computer Science and Communication
Department of Media Technology and Graphic Arts
SE-100 44 Stockholm, Sweden

Topographical micro-changes in corrugated board production
Effects on flexographic post-print quality

Study was carried out at
STFI-Packforsk AB
Drottning Kristinas Väg 61
SE-114 86 Stockholm
Sweden

Photos on page 7, 17, 41 and cover – © Martin Burmester
Photos on page 1, 21, 31 – © Marcus Rehberger
Photo edit: Martin Burmester

TRITA-CSC-A 2007:21
ISSN 1653-5723
ISRN KTH/CSC/A--07/21--SE
ISBN 978-91-7178-824-5

Royal Institute of Technology – KTH
School of Computer Science and Communication
Department of Media Technology and Graphic Arts
SE-100 44 Stockholm, Sweden
www.kth.se

Thesis for the degree of Licentiate of Technology to be presented with
due permission for public examination and criticism in Room D41, Lindstedtsvägen 3
at the Royal Institute of Technology, KTH,
on 14 December 2007 at 10.00.

Printed 2007 by Universitetsservice AB, Stockholm, Sweden

Dedicated to my beloved grandmother
Gewidmet meiner geliebten Oma
Anna Schmöller

Abstract

The appearance and design of a package are key properties to attract and to focus the attention of a customer. Print quality contributes to a great degree to achieve these requirements. Most critical perceived in terms of quality are print defects like mottling, gloss and stripiness, which all appear in the printing of corrugated board. Stripiness is especially critical because it is a defect directly caused by the corrugated board construction. A further cause can be generated by the production process of corrugated board. Pre-studies by Odeberg Glasenapp (2004) revealed a difference in surface micro-roughness between the regions on the peak line of the liner and the regions in the valley between two peaks of the corrugation. This knowledge was the basis for the work described in this thesis.

In a first stage, laboratory trials were conducted with sets of coated and uncoated samples of various grammages. The trial was set-up in order to simulate the conditions in the corrugator as closely as possible. In the evaluations, it was found out that the settings were too high. For that reason, the coated samples were influenced to a too high degree and needed to be excluded from further evaluations. With the uncoated samples, on the other hand, a change in micro surface roughness was detectable. The roughness is decreased on the peaks and the gloss appearance was the conclusion. The analysis of the printed samples focused on shifts in colour and print density. It is unclear if both are affected only surface roughness changes and/or by the typical corrugated board effect of washboarding.

A full-scale test was performed in order to confirm the results of the laboratory test. A test series was chosen with coated and uncoated outer liners. Contrary to the lab-test results, the uncoated grades showed no surface roughness changes. Instead, the coated samples were affected to a great extent. The changes in surface roughness and gloss appearance were similar to the lab-test. This confirms that the lab-test samples were exposed to heat, pressure and shear to a too high degree. The print analysis of the full-scale test did not agree with the laboratory test. Gloss lines were visually detectable, but they were difficult to measure. A reason could be that the ink is capable on forming an ink film layer on top of the surface of the paper. This would cover the micro roughness of the matt parts thereby creating an almost homogeneous glossy appearance.

Keywords: corrugated board, liner, double-facer, double-backer, gloss, surface roughness, micro structure, wear, paper metal friction, flexo, ink-jet, print quality

Preface

Mahatma Gandhi once said “My life is my message” and my message is now what is lying in your hands and you are about to read. In two years I have wallowed through articles and books, made the laboratory my second home and dug through a huge mountain of produced data. I did not even stop to keep my hands off giant machines like a corrugator. But something more enriched my experience. Something continuously is challenging me. Presenting my work in front of an audience and to collaborate with the industry. Now I “love” it and in addition, it helps me to reach one of my old dreams, to visit the world.

I would not be where I am now, at the Swedish Pulp and Paper Research Institute (STFI-Packforsk AB) and finishing my Licentiate degree, if some very important persons had not supported me to such a great extent. One of them is Dr. Astrid Odeberg Glasenapp. She continuously opened new doors for me and supported me wherever she could; thank you Astrid for all. I was lucky, because she was not my only great supervisor. Dr. Per-Åke Johansson was my mentor for all questions with a theoretical background and without him, I would have got lost in the deep forest of equations. Last but not least my supervisor at KTH, Prof. Nils Enlund, thank you for all your academic guidance.

I wish to express my appreciation to the industrial partners in the STFI-Packforsk AB cluster FuncPack for their financial support. Moreover, Sören Persson (Miller Graphics, Sunne, Sweden), Joris Haems (HP Scitex, Belgium) and Jürgen Bäuml (BHS-Corrugated, Germany) for their generous support.

My colleagues at STFI-Packforsk are acknowledged for fruitful collaborations.

Good friends are the precious well for a happy and successful life. None of my friends I would like to miss. Thanks to all of you.

Zu guter Letzt möchte ich meiner Familie für Ihre unaufhaltsame Unterstützung danken. Wo wäre ich nur ohne euch?

Stockholm, Sweden, November 2007

Marcus Rehberger

List of Papers

Paper I

Rehberger, M., Odeberg Glasenapp, A., Johansson, P.-Å. and Gällstedt, M. (2006)

Topographical micro changes of corrugated board liners induced by heat treatment and their effect on flexographic print quality. In Advances in printing and media technology: proceedings of the 33rd international research conference of Iarigai. Leipzig, Germany.

Paper II

Rehberger, M., Odeberg Glasenapp, A. and Johansson, P.-Å. (2007)

Topographical micro-changes on corrugated board liners - A comparison between laboratory and full-scale effects. In 59th Annual Technical Conference of TAGA. Pittsburgh, Pennsylvania, USA.

Paper III

Rehberger, M., Odeberg Glasenapp, A. and Johansson, P.-Å. (2007)

Corrugated board production and its micro-scale impacts on the liner's topography. In VIIIth Seminar in Graphic Arts. Pardubice, Czech Republic.

Time Line

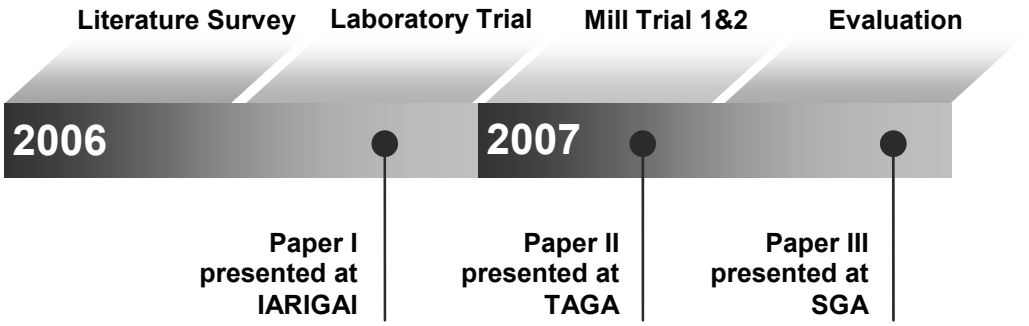

Content

1 Introduction

1.1 The 5 dimensions of human senses

Human beings interact with products at the Point of Sale (PoS). Here, the decision "shall I buy this or not" takes place. The buying decision consists of five dimensions: seeing, hearing, touching, tasting and smelling, but most companies are thinking only two dimensionally and forget the last three senses (IRI, 2006, VDW, 2006). The result of a study performed by IRI shows that different products activate different senses and the more senses are activated the higher will be the product loyalty. Which of these multi-sensor components is activated is dependent on the product (figure 1). Detergents for instance are judged by their smell, and sweets packages have to catch the eye. To follow such rules could be helpful, but sometimes it could also be useful to breach the rules and try something else. Nevertheless, as illustrated in figure 1, the visual appearance and the sense of seeing is the most crucial element.

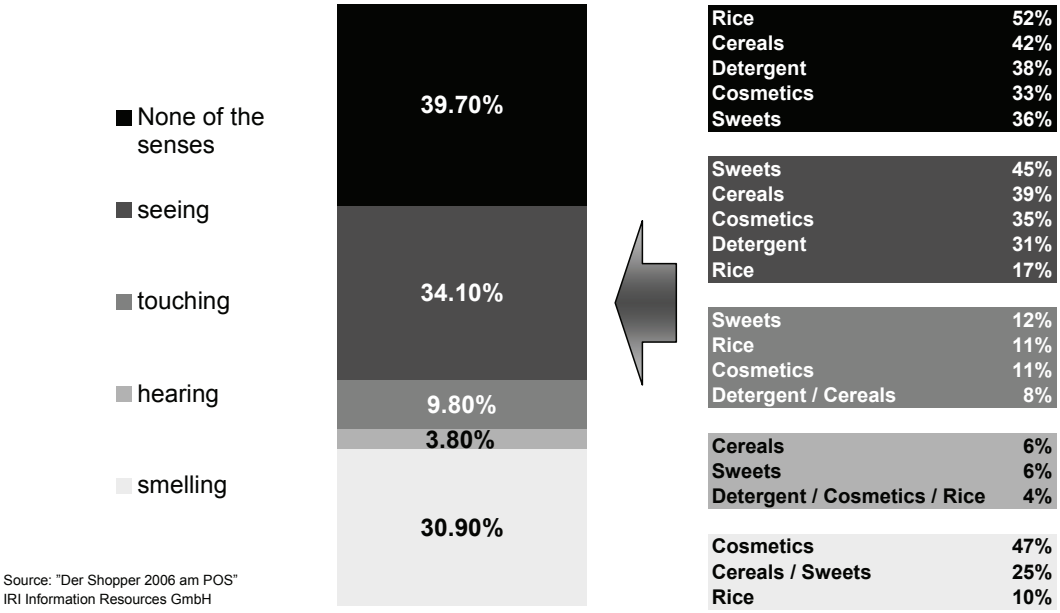

Figure 1 *The importance of different senses for the buying decision at the PoS.*

Many factors can influence the "buying" decision at the PoS. The most decisive factor is the quality of the product, which goes along with the brand (figure 2). However, not that far behind is the information about the product on the packaging and there after comes the packaging itself, influencing the buying decision. The trend nowadays is to present the product together with its packaging. Electronic stores are good examples, because they advertise their products in most cases on top of their own packaging, like printers, laptops and so on. Even when the product is not positioned on its own packaging, it is placed nearby and visible for the customer.

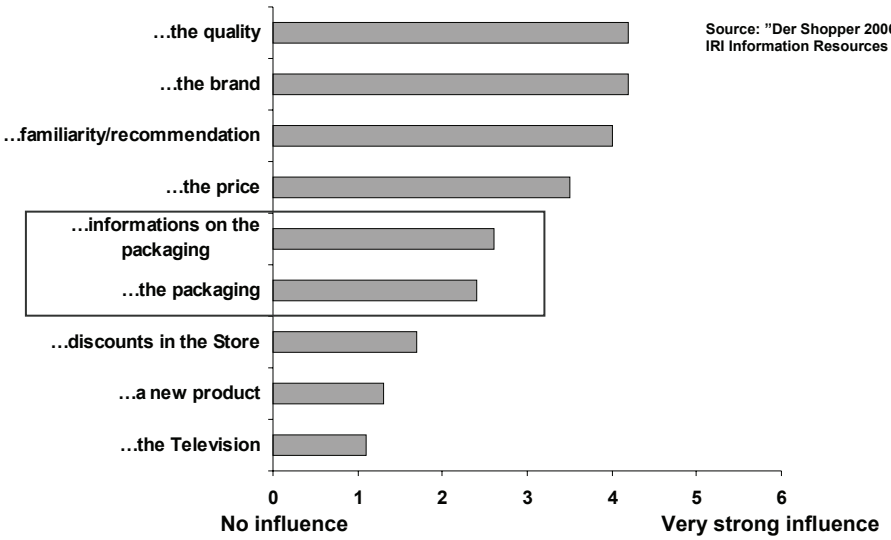

Figure 2 *The factors most influencing the buying decision.*

This trend is leading to greater requirements on the packaging producers and on the printing industry. The "packaging" is influencing the buying decision to a great extent. Yet, some producers still believe that packaging printed in a single colour is enough to catch the attention of the costumer. This would be true if the packing were not at the Point of Sale (PoS) and becoming a purchase criterion. If the product is at the PoS, the demands on the packaging increase dramatically. Beside the need to keep the goods safe, it also has to address most of the human senses and primarily the eye to attract customers. This fact requests a lot of effort in the corrugated board industry. Most corrugated board sheets are printed in flexo post-print and this involves several difficulties; the most important of which is discussed in the following paragraph.

1.2 Stripiness in flexo post-print

Periodical print defects, such as stripes, on a corrugated board package are a serious problem as they are more easily perceived than random print defects (Netz, 1996). Stripiness has many origins and one of the most frequently discussed is washboarding. Washboarding is a macro-scale defect and is the result of the wave-formed structure of the corrugated board liner (Barros, 2006, Cusdin, 2000, Holmvall, 2007, Netz, 1996, Odeberg Glasenapp, 2004, Pedraza, 1993, Zang et al., 1995). In the printing unit, this wave-formed substrate surface leads to sections with overpressure (peak) and areas with too little pressure or without any contact with the printing plate (valley). The result may look like a stripy print as illustrated in the right position in figure 3. On the other hand, stripiness can occur even without any washboarding appearance. In that case, it is called induced stripiness. This means that during the printing process and only when pressure is

applied, the liner forms a wavy structure. Afterwards, the board appears to be perfectly flat again, but with stripes in the print. In figure 3 (left), the forces during the printing process with washboarding are illustrated.

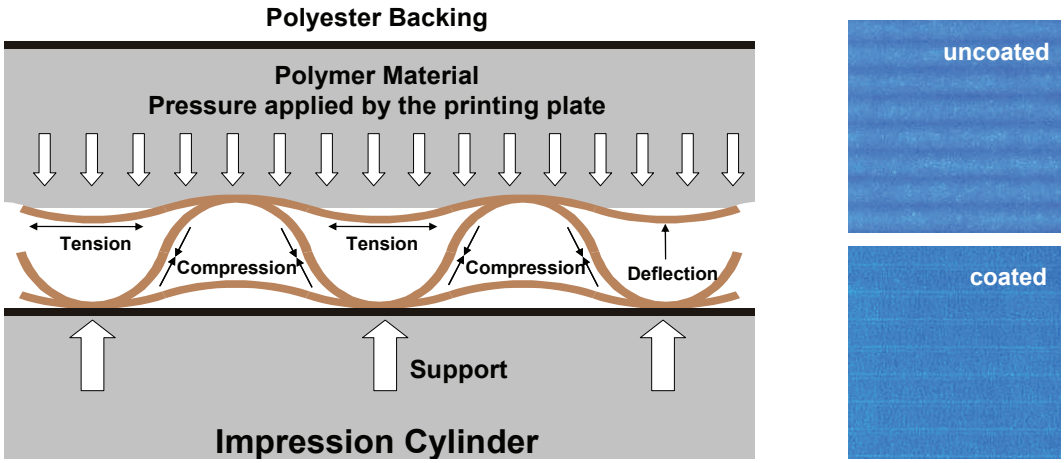

Figure 3 *Left: Origin of stripiness in flexographic post-print in theory (Cusdin, 2000); Right: Real examples of flexo-printed corrugated board with stripiness; top: uncoated with washboarding; bottom: coated without washboarding, but still with a striped print (Rehberger, 2004)*

Netz (1996) describes three different types of stripiness. Washboarding is the most common reason for stripiness. Second but less common type is inverted stripiness where, in contrast to the common stripiness, the brighter stripes are on the flute peak line. The origin is print density differences due to liner absorption differences. The third type is stripiness of pre-printed board where the print is damaged by the corrugating process. In addition there is a fourth effect. If there is washboarding, our effect of stripiness is created through shadowing effects due to different light incident angles

There are different types of stripiness in flexographic post-prints on corrugated board affect the observer's judgement differently (Lindberg, 2004). Not only is the existence of stripiness crucial for how it is judged. For instance, the frequency of the stripes adds further complexity to the context.

1.3 The origin of the work

The work described in the thesis began with studies performed by Astrid Odeberg Glasenapp (2004). Besides measurements of the cross-section of the corrugated board, a chapter about *"micro-structure of corrugated board liner"* was included. The topographical tests were carried out on uncoated White Top Kraftliner using AFM (Atomic Force Microscopy) and CLSM (Confocal Laser Scanning Microscopy). The outcome was that the surface roughness had changed in micro-

scale on the peak of the outer liner. Sections located on the valley changed to a lesser degree. Shifts in surface roughness between peak and valley and between peak and raw material were measured. The reasons behind this phenomenon were quite unexplored and no clear explanation could be given. The source of this effect, however, must be located in the production of corrugated board. The present work has been aimed at obtaining a greater understanding of these effects and their consequences in post-print.

1.4 Conditions in the double-backer of the corrugator

The most common corrugated board (CB) consists of three layers, an inner liner, a fluting layer and a outer liner. These layers are linked by glue bondings at each tip of the fluting medium. Depending on the application, numerous combinations between liners and fluting medium are conceivable. In addition, each different CB type needs separate settings of the corrugator such as temperatures, glue gap, wrapping angle.

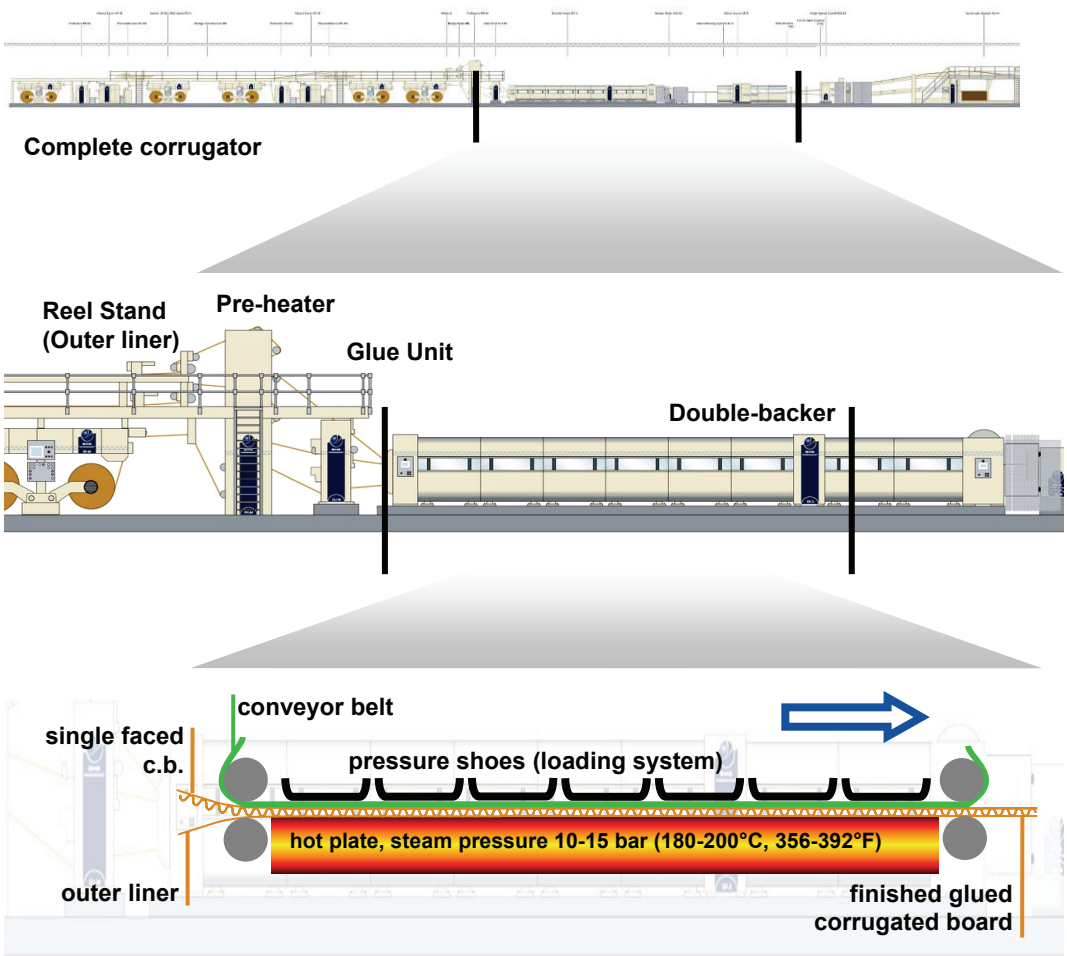

Figure 4 *Overview of the corrugator; top: complete corrugator; middle: from reel stand outer liner till end of double-backer; bottom: scheme of double-backer (Schematics of corrugator: © BHS-Corrugated)*

Many variables drive the corrugator and create many different problems. Warping, washboarding and poor bonding are "only" three of them. Since the problems arise on the printing outer liner, influences cannot be induced before the outer liner enters the production process, i.e. behind the reel stand for the outer liner and just before the pre-heater and the double-backer (figure 4). The further processing includes cutting and stacking. Stacking is known to affect the substrate surface quality, too, but this factor can be avoided by extracting the samples right after the cross cutter. The conditions, which occur in the double-backer, are far from optimal for papers or paper coatings. Hot plates with temperatures up to 200°C combined with a pressure load from the top are needed to cure the glue and to ensure proper bonding (Mensing, 2006, Pinnington, 2003). In addition, paper-metal friction occurs, because the CB is pulled over the hot plates made of steel. The double-backer section may be the section that has the strongest impact on a paper surface, cf. Odeberg Glasenapp (2004).

2 Theoretical foundation

2.1 Paper-Metal Friction

Tribology (from greek tribo, meaning I rub) explains the interaction between solid surfaces in relative motion (Persson, 2000). This is called sliding friction and the fundamental equation describing this case is the Coulomb's friction law:

$$F = \mu \cdot L \qquad (2.1)$$

where

F = friction force

μ = coefficient of friction

L = load (normal force).

Friction is basically independent of surface roughness and surface contact area. However, in the case of paper-to-metal friction, the friction increases with increasing metal surface roughness (Back, 1991). The harder, rough surface particles of metal are grinding or even ploughing into the softer paper material.

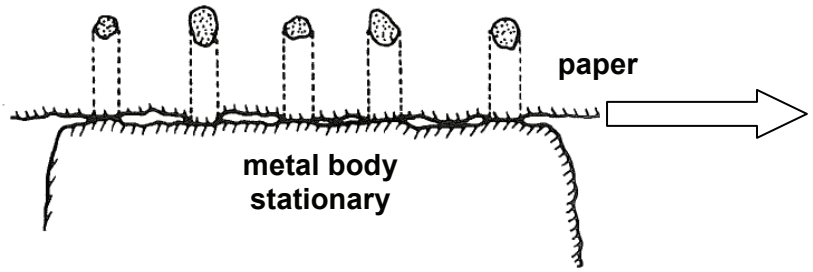

Figure 5 *Schematic illustration of paper-metal contact, showing a large apparent area and smaller real areas of contact (Persson, 2000)*

Figure 5 illustrates the contact between a paper and a metal plate. The small circles above the paper show the real contact area in contrast to the "apparent" contact area, which is defined by the dimensions of the objects. The friction coefficient is thus very dependent on the difference in hardness between two gliding objects and not only on too rough or too smooth surfaces, as described by Persson (2000).

2.2 Surface reflection

Reflection is the change in direction of a ray of light when it strikes a mirroring surface (figure 6). The incident light beam and the specular reflected light beam lie in the same plane (Hering et al., 1999). Refraction of the light beam occurs in the same layer, but the refraction angle θ_t is dependent on the difference in refraction indices of the medium (n_2) and the air (n_1).

$$\frac{\sin \theta_i}{\sin \theta_t} = \frac{n_1}{n_2} \qquad (2.2)$$

where

θ_i = incident angle of the light beam

θ_t = refraction angle of the light beam

n_x = different mediums

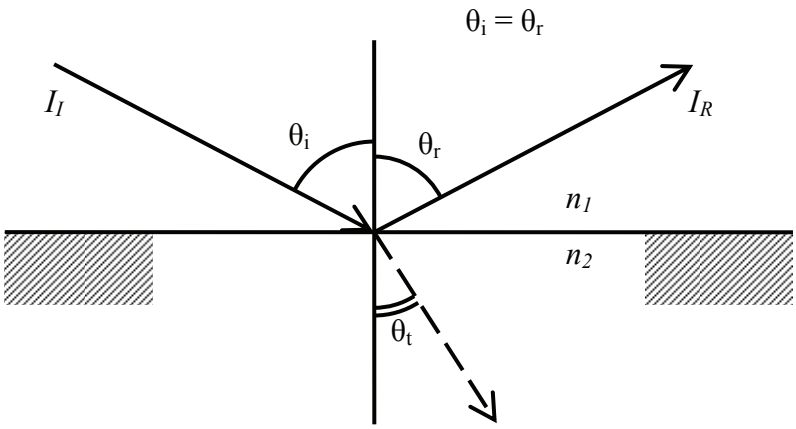

Figure 6 *A ray striking the interface between two media is split into a reflected part and a refracted part (Louman, 1983); the reflection angle θ_r is equal to the incident angle θ_i; the refraction angle θ_t is calculated with the formula above.*

The theory behind reflection is described with the Fresnel equations in conjunction with light reflexion on non-metallic surfaces.

$$R_0 = \frac{I_I}{I_R} = \frac{\rho_s + \rho_p}{2} \qquad (2.3)$$

where

R_0 = reflectance

I_I = incident ray

I_R = reflected ray

$\rho_s = \left[\frac{\sin(\theta_i-\theta_t)}{\sin(\theta_i+\theta_t)}\right]^2$ polarised perpendicular to the plane

$\rho_p = \left[\frac{\tan(\theta_i-\theta_t)}{\tan(\theta_i+\theta_t)}\right]^2$ polarised parallel to the plane.

As Louman (1983) indicates, these equations are valid only for perfectly plane and closed surfaces. Paper surfaces are never perfectly plane. Furthermore, as Bennett (1999) states, the surface is assumed to be opaque. Effects such as light transmitting into the material, scattering by material defects, or reflected from the back surface, are neglected. In addition it is assumed that the reflection angle is exactly equal to the incident angle. The following equation is adapted for rough surfaces and inclined incidence of light (Bennett et al., 1999, Johansson, 1999, Louman, 1983):

$$\frac{R_S}{R_0} = \exp\left[-\left(\frac{4\pi\sigma\cos\theta_i}{\lambda}\right)^2\right] \qquad (2.4)$$

where

R_S = specular reflectance of a rough test sample

R_0 = specular reflectance of a perfectly plane surface

σ = rms surface roughness (R_q)

θ_i = angle of incidence

λ = incident wavelength.

With this reflectance formula, the reflection dependent on the incident angle and on the roughness can be calculated. In the case of corrugated board, the following equation can be used to derive the contrast k between the gloss from the peak and valley of the liner surface.

$$k = \left[\frac{\left[R_S/R_0\right]_{peak}}{\left[R_S/R_o\right]_{valley}}\right] \qquad (2.5)$$

where

k = contrast in reflectivity between peak and valley.

Technically gloss is an effect of specular reflectivity on surfaces. In terms of print quality, this is a major factor affecting human perception (Béland et al., 2000, Lindberg, 2004, Lindstrand, 2002). The contrast value k is a measure of the

difference between two different surface regions. The higher the value k the higher will be the gloss contrast effect and thus the visual disturbance.

2.3 Print density and Colours (L*a*b*)

Density measurements

The optical print density is calculated as the logarithm of the ratio of the reflection of unprinted base paper to the reflectance factor of the printed substrate.

$$D = \log \frac{R_0}{R} \qquad (2.6)$$

where

D = density

R = reflectance factor of the printed area

R_0 = reflectance factor of the blank substrate

A densitometer is calibrated with an unprinted reference for which the density D = 0. Increasing ink-film thickness decreases the remission and the density increases (Brehm, 1992). The principle of the density measurement is illustrated in figure 7.

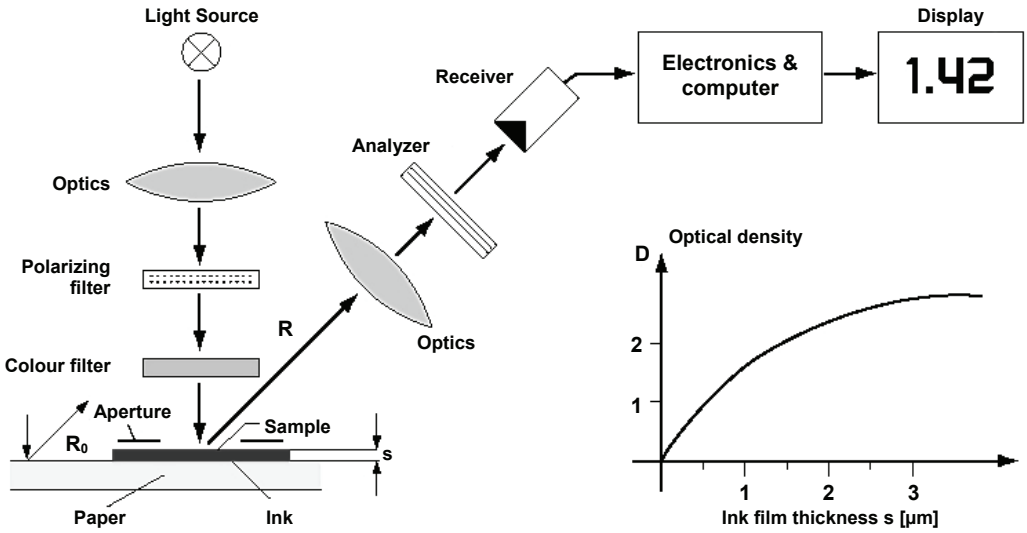

Figure 7 *Principle of the density measurement; chart to the right illustrates the relation between optical density and ink film thickness (Source: Kipphan, 2001)*

Colour measurements

The CIELab colour space was defined by the Commission Internationale de l'Eclairage (CIE) in 1976. This 3-dimensional colour-space has three axes as illustrated in figure 8. The mathematical model behind is illustrated in the following equations.

$$L^* = 116\left(\frac{Y}{Y_n}\right)^{1/3} - 16 \qquad (2.7)$$

$$a^* = 500\left[\left(\frac{X}{X_n}\right)^{1/3} - \left(\frac{Y}{Y_n}\right)^{1/3}\right] \qquad (2.8)$$

$$b^* = 200\left[\left(\frac{Y}{Y_n}\right)^{1/3} - \left(\frac{Z}{Z_n}\right)^{1/3}\right] \qquad (2.9)$$

where

L^*	=	Luminance
a*, b*	=	colour-opponent dimensions
X, Y, Z	=	CIE tristimulus values
X_n, Y_n, Z_n	=	tristimulus values of the neutral white

L* is the lightness of a colour and can be between 100% (white) and 0% (black). In the a*b* coordinate system the a* axis represents the red / green components and the b* axis the yellow / blue components (Pauler, 2002). The knowledge about the exact colour values is not always the most important part. Furthermore, a significant factor is the colour difference between a reference and a sample. For that reason CIE introduced together with the L*a*b*-space in 1976, the ΔE value and the higher the value, the greater is the difference between two colours:

$$\Delta E_{ab} = \sqrt{\left(\Delta L^{*2} + \Delta a^{*2} + \Delta b^{*2}\right)} \qquad (2.10)$$

where

ΔE_{ab}= colour difference between two samples

$\Delta L^* = L_1^* - L_2^*$

$\Delta a^* = a_1^* - a_2^*$

$\Delta b^* = b_1^* - b_2^*$

CIE introduced an improvement of the calculation in 1994 and a further improvement in 2000. These equations are meant to match the visual judgement more closely, but they are more complex to calculate. The equation from 1976 is sufficient for an overview of the colour difference between two samples in a printing contrast.

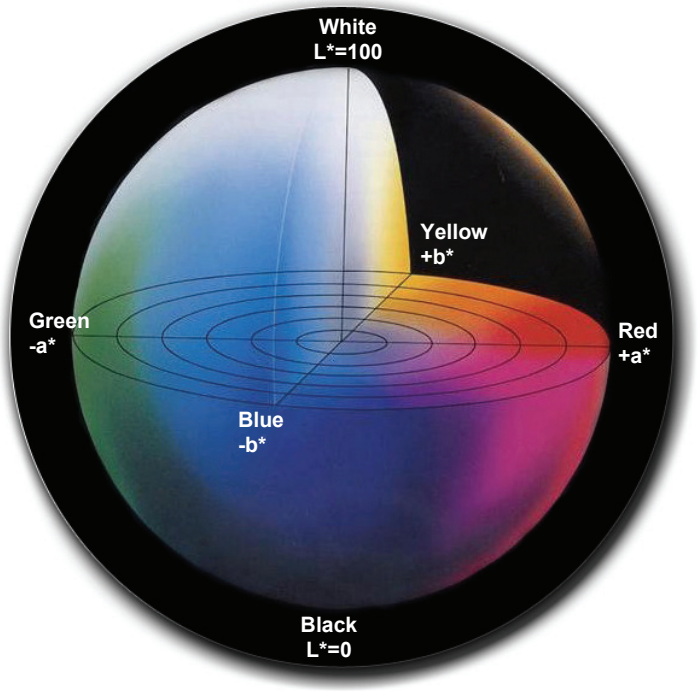

Figure 8 *The CIELab colour space with the axis a*b* for colour and L* for lightness. (Note: sphere illustrates not the real shape of the L*a*b* colour space)*

3 Methods

3.1 Topographical measurements

CLSM (Confocal Laser Scanning Microscope)

The Confocal Laser Scanning Microscope Radiance® 2000 (Bio-Rad Laboratories, USA), equipped with Kr/Ar laser, can be used to investigate the micro-roughness of liner surfaces with a 200 x magnification. Roughness measurements can be conducted by indirect or direct methods such as surface profilometry. CLSM offers a non-contact method for surface profilometry like the FRT MicroProf. The technique is especially suitable for the evaluation of microscopic roughness (Moss et al., 1993). The CLSM was used to obtain images of the surface in higher magnification and to verify the MicroProf results.

AFM (Atomic Force Microscopy)

Multimode® NanoScope® IIIa from Veeco Instruments Inc. (Woodbury, NY, USA) is a tool capable of scanning surfaces on the atomic level. It captures images of a maximum size of 100x100 µm and a z-direction working range of 6 µm. A measurement head oscillates over the surface and measures the normal and lateral deflections. This gives information about the topography and material properties, such as elasticity

FRT-MicroProf®

FRT-MicroProf® (Fries Research & Technology GmbH, Germany) is used to investigate the topography of a scanned surface. It is a non-contact method and surface height profiles indicating roughness and waviness can be acquired. Its principle (figure 9) is based on chromatic aberration where white light is split up into different colours focused on different heights. The light reflected by the surface is analyzed and the data are computed into a topographical image.

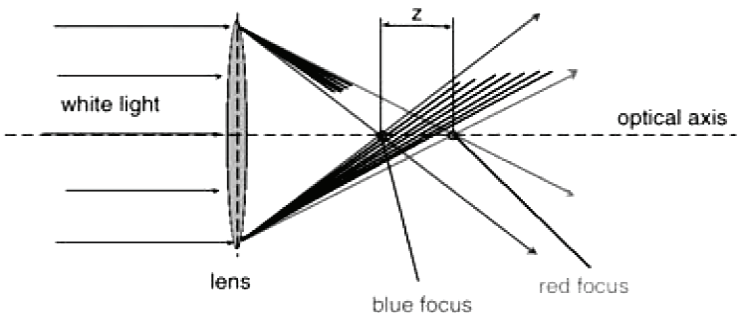

Figure 9 *The principle of the FRT topography meter MicroProf (Source: © FRT GmbH)*

3.2 Printing

Flexographic printing (IGT F1 Printability tester)

Historically, flexography can be traced back to letterpress and since then printing flexographic has developed increasingly. Flexo-print is in principle comparable with printing with a stamp; the ink is applied on the raised layout and transferred to the substrate. In the packaging industry and especially for corrugated board, two types of flexo-print exist, pre-print and post-print. First one implies that the substrate is printed before the corrugated board is produced. Post-print on the other hand means that the print takes place after the production process.

In this work, the printing was performed with an IGT F1 laboratory printing-machine (IGT Testing Systems, Amsterdam, Netherlands). The IGT F1 consists of an inking unit with anilox roll and doctor blade and a printing unit with a printing form on a cylinder (figure 10). The printing width is 50 mm and the perimeter of the printing form is 534 mm with a diameter of 170 mm.

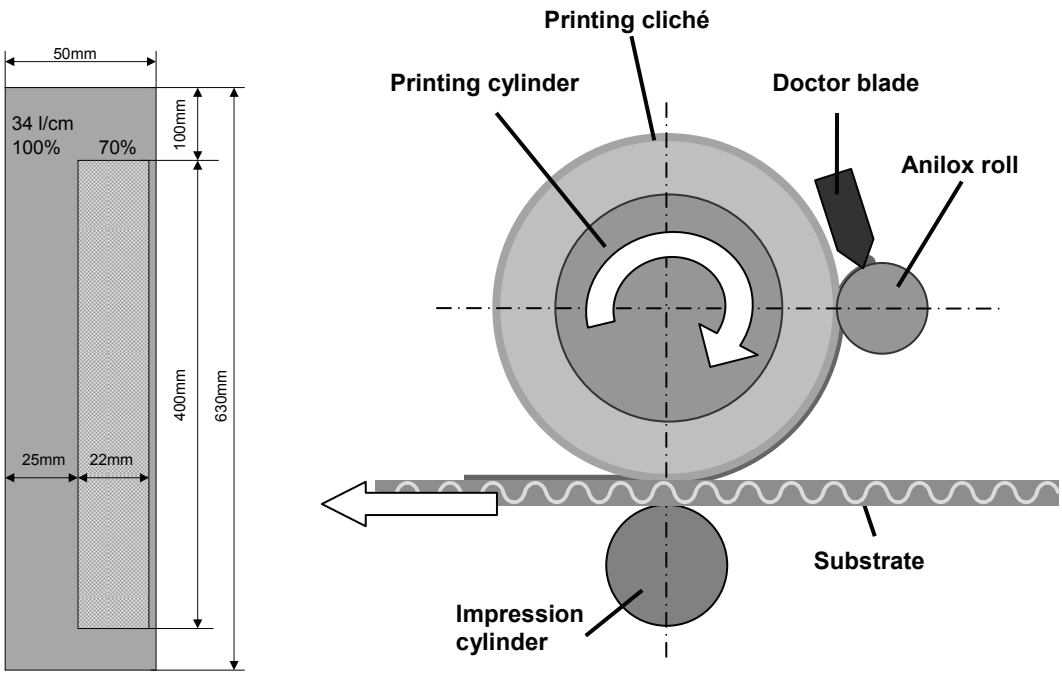

Figure 10 *The IGT F1 Flexo Tester; design of the printing cliché (left) and a schematic overview of the IGT-F1 flexographic printing machine (right).*

Ink-jet printing

Flexo-print is an "impact print" method. The printing cylindar touches the surface of the substrate during the printing process and applies pressure to it (Kipphan, 2001, Meyer, 1999). Printing without impact provides information about surface

changes due to the impacts in the printing of corrugated board. Such methods are called “non impact printing” (NIP) and the best example is ink-jet printing. The ink is expelled in the form of droplets from the printing head before it meets the surface of the substrate. Depending on ink, substrate and further processing, different drying methods are used, like UV- or IR-curing. In packaging printing, ink-jet printing develops new possibilities, like customized print, new types of substrates and non-damaging influence on the substrate.

The ink-jet printing for this work was performed at HP Scitex (Zaventem, Belgium) with the HP Scitex FB6700. The printing head from Aprion is able to accelerate 25,000 droplets/sec/nozzle, has a resolution of true 600dpi and works in FM mode (stochastic). It prints with HP Scitex WB300 Supreme ink, which is a pigmented water-based ink, and the machine can be filled with the colours C, M, Y, K, Light Cyan (LC) and Light Magenta (LM). For the test, only Cyan was used.

3.3 Surface and print analysis

STFI-MicroGloss

The effect of gloss on unprinted or printed surfaces can be measured with the STFI-MicroGloss meter (Johansson et al., 2004). It captures images from the sample using illumination and camera angles of 20°/20° (figure 11). The programme is able to make single images or a matrix of images. Both were used, because some samples were too small for an image matrix. A single image has a size of 13x13 mm and the stitching process was performed with Adobe® Photoshop®.

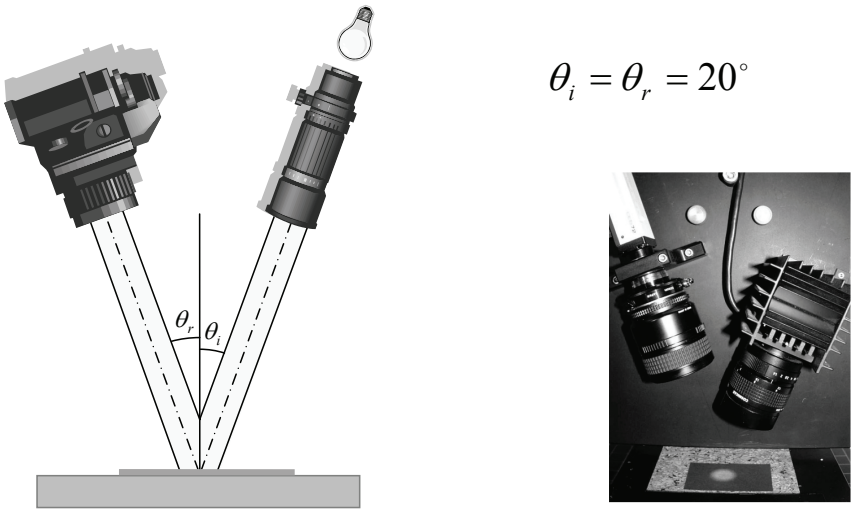

Figure 11 *Construction of STFI-MicroGloss meter (Johansson et al., 2004).*

In addition was set up for the full-scale test a provisional testing with incidence and reflecting angle of 45 degrees. The test setup was similar to that illustrated in figure 11 with an illumination through an objective striking the sample surface. The recording instrument was here a photo-camera and not a CCD-camera.

Print density and L*a*b*

The printed samples were measured with the 938 – Spectrodensitometer (X-Rite®, Grandville, MI., USA). The range of the measured reflectance spectrum is 400-700 nm, at intervals of 20nm. The illumination angle of the test area is 0° and the viewing angle 45°. For the measurements, the response "E" was chosen, which represents a European response using the 47B filter for yellow.

The same instrument was used for the L*a*b* colour measurements. The settings for the measurements were chosen as follows, the L*a*b* (CIE 1976) colour space with the CIE 1931 2° observer and the D65 illuminant.

4 Tests on a laboratory-scale

4.1 Experiments

Preparation of samples

Planning and performing tests on a full scale in a corrugator can be very time-consuming and furthermore, the tests would be dependent on the daily production. Executing the tests on a laboratory scale instead is more flexible and quick changes in the test setup can be made instantly. Despite the advantages of laboratory tests, one disadvantage is that speed is a critical parameter. The top speed of actual corrugators can be 420 m/min; this can never be achieved on a laboratory scale. On the other hand, a laboratory trial should not produce corrugated board comparable to real sheets. It is more important to obtain an overview about which setting is the most significant one. The data from the tests can be compared with the data from the topographical tests and finally with the print results.

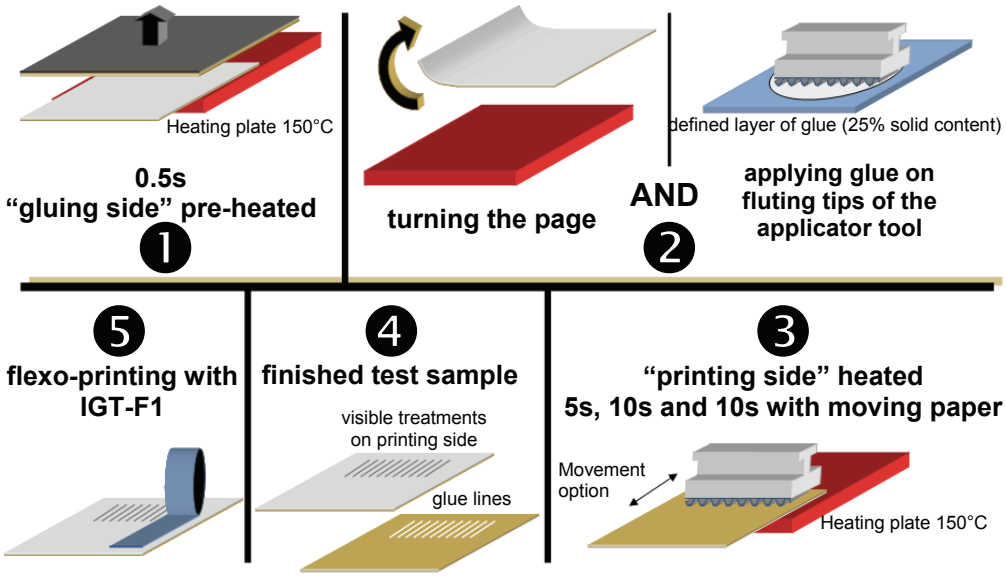

Figure 12 *Test procedure for producing differently treated samples.*

The laboratory trials are described in detail in Paper I. The tests reported in that paper focus on uncoated papers and further data for coated liners can be found in Paper II. The laboratory test (figure 12) was set up in order to comply with the procedures in a corrugator. These tests contain only the process steps from the reel stand of the liner to the end of the double-backer (figure 4). In the lab-test, the paper was pre-heated on the gluing side with a heating plate. After turning the sheet, it was loaded with a tool with a milled flute profile. This tool simulates the flute profile and the load from the double-backer top heating plates. In addition, glue was applied on the flute tips of the tool to include possible influence factors

like moisture and evaporation. During step 3, one set of liners (10sM) was moved back and forth on the laboratory heating plate, whereas for the other set (10s, 5s), this movement was omitted, in order to measure the difference between moved and unmoved paper on a hot plate. In addition, the chosen times on the heating plate were 5s (only unmoved) and 10s (both moved and unmoved). In a last step, the chosen samples were printed with a laboratory flexographic printing machine. This entire procedure was applied to a set of different liner grades, listed in table 1.

Table 1 *Overview of paper grades used for laboratory testing*

Code	Manufacturer	Type	Coating	Grammage
1u110	M 1	Pure White	uncoated	110 g/m^2
1u170	M 1	Pure White	uncoated	170 g/m^2
2u100	M 2	White Top	uncoated	100 g/m^2
2u175	M 2	White Top	uncoated	175 g/m^2
2s170	M 2	White Top	single coated	170 g/m^2
2d130	M 2	White Top	double coated	130 g/m^2
2d175	M 2	White Top	double coated	175 g/m^2
2d200	M 2	White Top	double coated	200 g/m^2

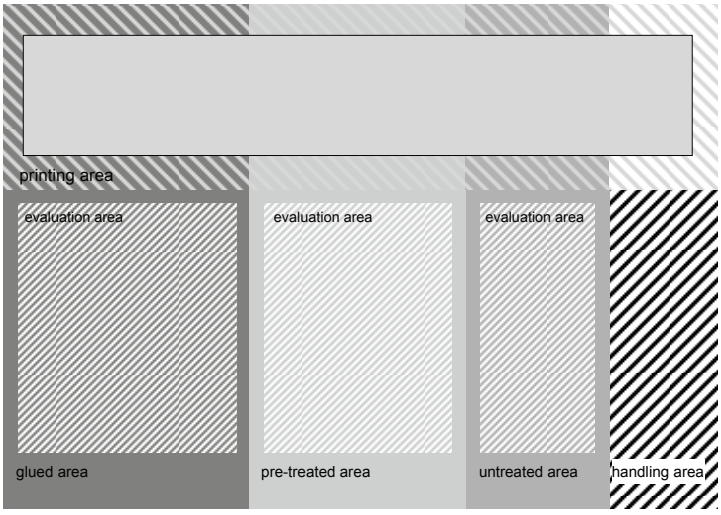

Figure 13 *Sectioning of lab-test samples for different measurements. Above the printing section, and below the unprinted section. From left to right: complete treated section, only pre-heated section and untreated part. A handling area was included to keep the rest of the section free from fingerprints.*

Due to variations in the paper production, it is possible that a paper roll can have different properties at the beginning and at the end and also from the right to the left side. Therefore, the test sheets were divided into several sections, printed and unprinted parts and areas with different treatments. The sections are described in detail in figure 13. The advantage is to have all the different treatment steps on one sheet so that variations due to paper production can be excluded. The final A4 sample sheet (step 4 in figure 12) showed in the "glued area" the treatment in form of washboarding and accordingly the glue lines on the reverse side.

Flexographic print

In order to optimize the print result, pre-prints were made. The settings with the IGT-F1 Flexo Tester, illustrated in table 2, gave the best print quality results. In this table, only the settings for uncoated grades are illustrated. Further explanation is given in the chapter "Results".

Table 2 *Overview of printing parameters used for uncoated paper grades.*

Variable	Settings for uncoated qualities
IGT-F1	Printing force = 50 N
	Anilox force = 35 N
	Printing speed = 0.6 m/s
	Revolutions = 2
Anilox roll	Cell volume 4.5 ml/m²
	Angle 45°
	Resolution of 140 l/cm
	IGT-Ref.no.: 402.208
Printing cylinder	Cylinder-Ø 166 mm
	Tape 0.55 mm (DuploFLEX 5.3, Lohmann)
	DuPont DPC digital cliché t = 1.7 mm 40 Shore A
Ink	SunChemical, diluted with demineralized water and adjusted to 21 s with DIN Cup #4

4.2 Results

Topography

The measurements with FRT-MicroProf, used for the laboratory trials, have been performed at a resolution of 10 x 1000 pixels in a range of 1 x 5 mm leading to a resolution of 5 µm in the y-direction (i.e. the flute direction). The z-direction

resolution is better than 10 nm. Figure 14 shows both coated and uncoated qualities. In these tests, the test rows with the moved samples (10sM) on the hot plate are crucial, because they are closest to the real case.

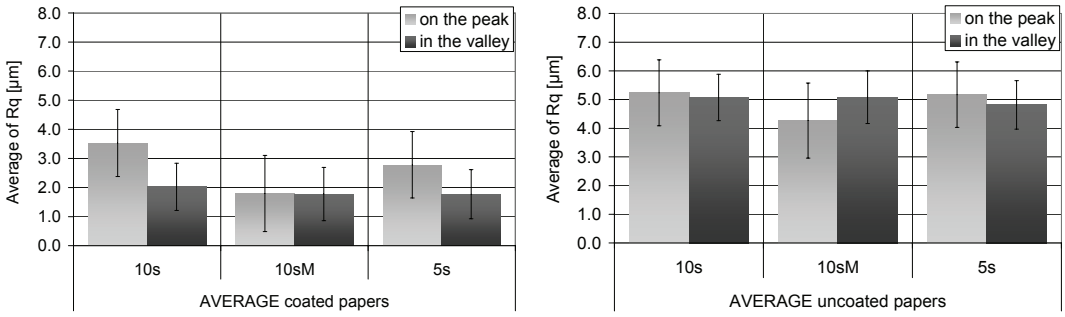

Figure 14 *FRT MicroProf results for coated and uncoated qualities.*

The uncoated 10sM-samples are showing a difference in surface roughness between peak and valley, while no difference is visible for the coated 10sM samples. Both valley and peak values of the coated sample were decreased compared to the reference. The gloss images in figure 15 support this statement, where this area-wide surface impact of raised gloss on the coated surface is visible. This fact was the reason to exclude the coated liners from further investigations.

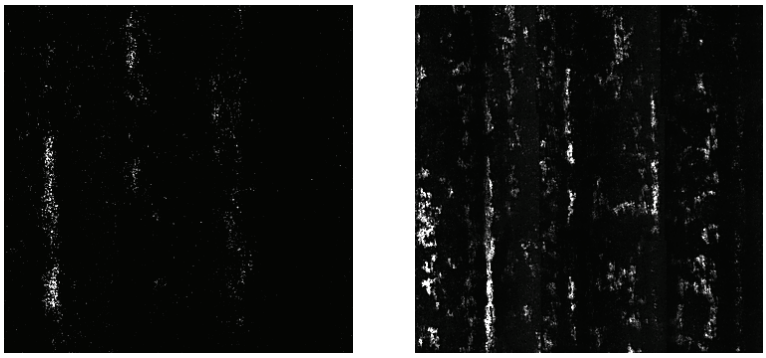

Figure 15 *Gloss results taken from the sample 2u175 (left) and 2d130 (right)*

The uncoated qualities, on the other and, are showing a clear result. The surface roughness for sample 10sM on the peak has decreased compared to the valley. This is confirmed by the gloss image of the uncoated sample. In addition, this image can explain the high standard deviation for the surface roughness results. The surface change is not uniform; some peak lines are affected more than other lines. Furthermore, the gloss lines are not uniform, but look mottled. Due to that, the surface roughness values differ and therefore a higher amount of measurements needed to be performed.

FRT MicroProf is showing reasonable results, but to get a more accurate statement, CLSM measurements were conducted. The uncoated quality "2u175" was chosen for the further measurements. Images in figure 16 are showing a change in the top fibre layers. The fibre structure of the peak area is extremely compressed in the top layers. The areas in the valley are affected too, but not to the same extent as the peak. Figure 17 confirms these visual statements with numbers.

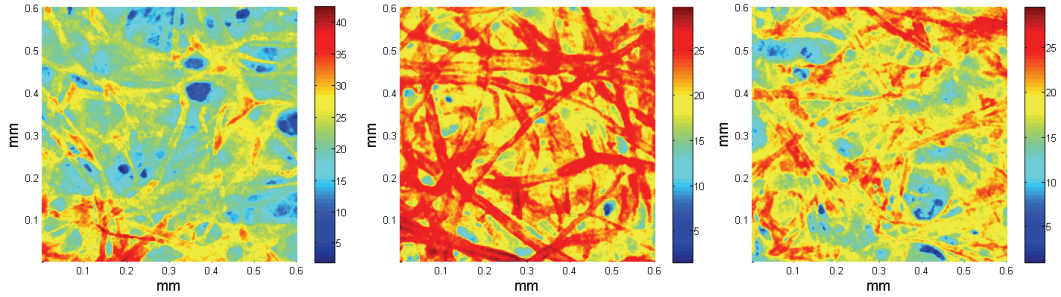

Figure 16 *CLSM images from sample 2u175; left: reference; middle: on the peak; right: valley*

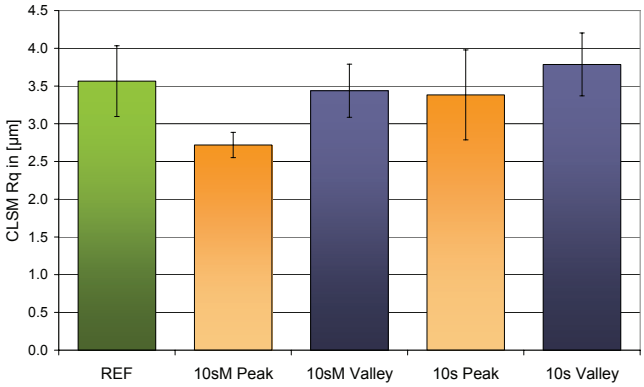

Figure 17 *CLSM results from sample 2u175 including the non-treated reference, the 10sM samples and 10s samples (from left to right).*

Print quality measurements

The evaluations of the laboratory test were continued only with uncoated grades. The printing layout included a fulltone and a 70% halftone, both of which were used for evaluations. The reference was the untreated and flexo printed part (see figure 13 and step 5 in figure 12).

The L*-value indicates the lightness of a colour. In figure 18 the surface difference between peak and valleys is especially visible in the halftones. The fulltone results are similar but the intensity is lower. The result leads to the conclusion that the peak is darker than the valley. The a*b* diagram (figure 19)

shows a shift in colour. The halftone peaks were more blue and slightly more green. The fulltones were completely different. In this case the peaks were less green. All the vectors had the same direction and the same length. In terms of colour difference, the halftones are affected the most (figure 20).

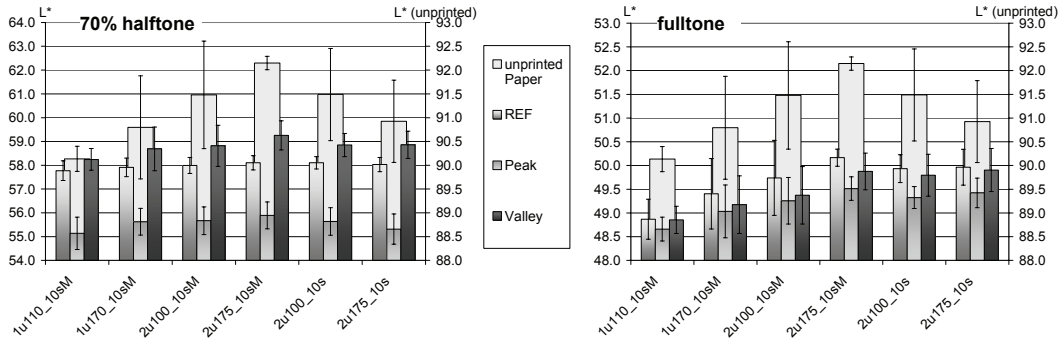

Figure 18 *L*-values of the uncoated qualities (left: halftone; right: fulltone); the bars at the front belong to the left-hand axis and the bars at the back to the right-hand axis.*

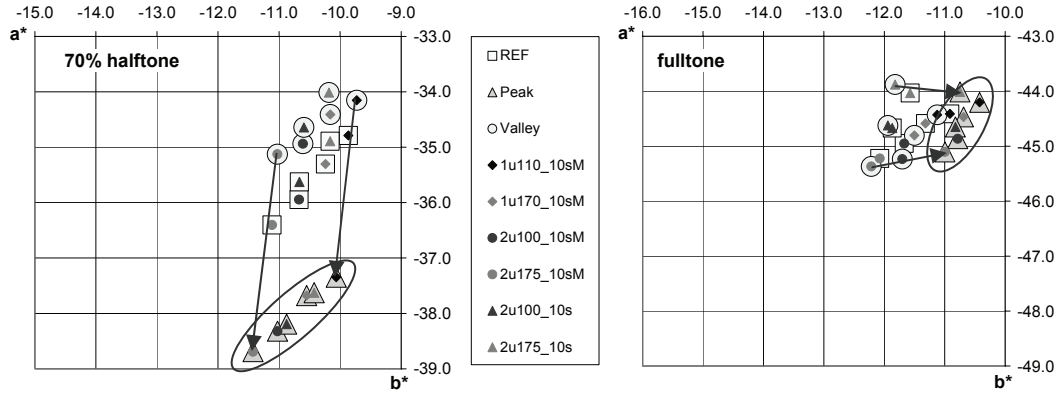

Figure 19 *a* b*-values; left the 70% halftone, and right the fulltone. The points enclosed in the ellipse are for the peaks and the arrows show the direction of the colour difference between peaks and valleys.*

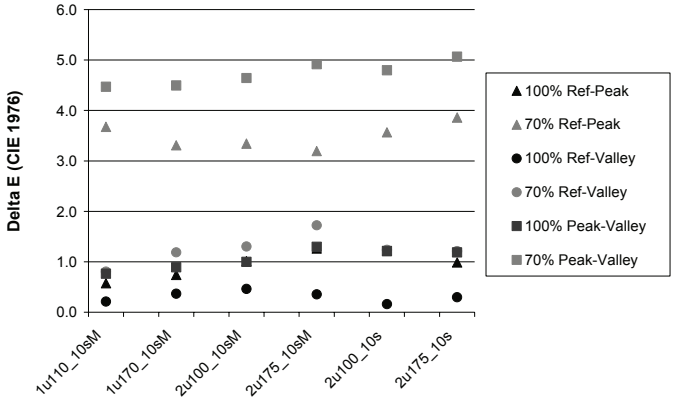

Figure 20 *ΔE (CIE 1976) differences between reference-peak, reference-valley and peak-valley, for both fulltone and halftone.*

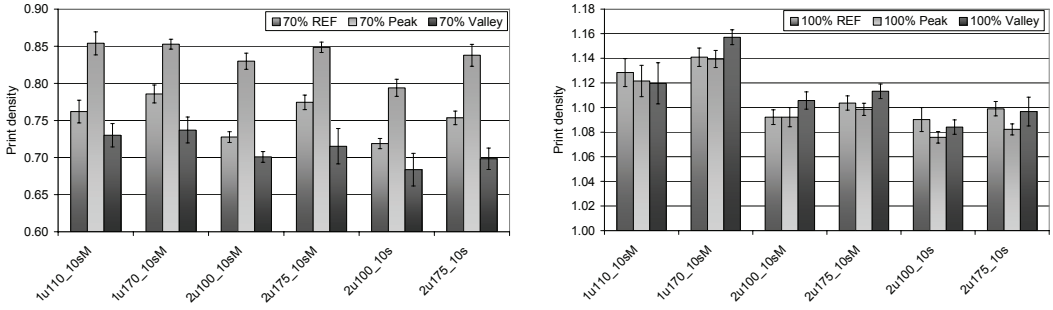

Figure 21 *Density results; left: 70% halftone; right: fulltone.*

The density was measured on both halftone and fulltone images. Figure 21 shows for the peak line values a higher density in halftone than the reference, but the values for the valleys are lower. In fulltone the results are different where shifts between peak areas and valleys are not clearly distinguishable. Only a difference between both paper manufacturers is given and to a minor degree between moved (10sM) and unmoved (10s) papers.

4.3 Discussion

In summary, it can be stated that the surface and the surface roughness was affected by heat, pressure and friction. There is no clear border between these factors; they are all interdependent. Furthermore was recognized, the higher the resolution of the topographical measurement system the more accurate was the results.

These surface changes are confirmed by the gloss measurements of the uncoated samples in terms of changed reflectivity behaviour between peak and valley areas. Similar images were captured of the coated samples, but the samples showed unexpected results. The coated samples were treated too harsh, leading to a substantial change in surface roughness. Parameters responsible could be too high pressure, too long treatment time and imperfect heating. It has to be assumed, that the top coating layer was rubbed off, especially at the peak lines. The uncoated grades were, however, less affected by these factors. This lets assume that the uncoated qualities are more resistant to heat, pressure and friction.

The prints were made with flexographic printing, which is dependent on the surface texture. Even though the samples were only single papers without fluting and second liner, the glue applied on the reverse side made the printing surface appear like a corrugated board surface with a washboarding effect. Washboarding may also have affected the print quality results in the laboratory trials. Stripiness and its background have been studied increasingly in the past few years by many researchers (Chalmers, 1998, Cusdin, 2000, Hallberg Hofstrand, 2006, Holmvall, 2007, Netz, 1996, Odeberg Glasenapp, 2004, Pedraza, 1993, Rehberger, 2004,

Zang et al., 1995). Two effects of washboarding are differences in print density and colour. For this reason, the results of the print analysis should be examined with caution. The printed colour on the peak area shifted in relation to the reference and the valley. In magnitude and direction, the shifts are dependent on the tone value, halftone or fulltone. The print density results were even more ambiguous if they belong to surface roughness results or not. Both print density and the colour measurements suggest a difference in ink film thickness. Especially in halftone, the peak lines appeared darker and the print density showed higher values compared to the valley region. The assumption if the print analysis results should be addressed whether to surface roughness changes or to washboarding effects, could not be clarified in this study.

5 Full-scale tests

5.1 Settings

Pilot Trial

The trials in the full-scale corrugator were divided into two parts, one for uncoated and one for coated grades (Table 3). In Paper II, the trials and the corrugator settings are described in detail. The settings (Table 4) for both trials were similar; they included changes in the pre-heater and double-backer temperature and in the production speed of the corrugator.

Table 3 *Overview of the paper materials used in the pilot trial*

Code	Outer liner	Fluting	Inner liner
Sxu	KL wTop 135 g/m^2	WS 170 g/m^2	TL 160 g/m^2
Sxc	KL dc 140 g/m^2	WS 110 g/m^2	TL w 140 g/m^2

KL: Kraftliner; WS: Wellenstoff; TL: Testliner; w: white; dc: double coated.

Table 4 *Machine settings for double-backer (DB), pre-heater (PH) and corrugator in general (WPA); variable "x" see code in table 3 (e.g. S1u or S4c).*

x	DB temp	PH temp	WPA speed
1	L	L	150 m/min
2	L	H	150 m/min
3	H	L	150 m/min
4	L	L	50 m/min

L: low temperature; H: high temperature.

Flexographic printing

The settings for coated and uncoated substrates were different to take into account different behaviours in terms of surface-ink interactions. When ink meets the relative closed surface of a coated paper, the pigments stays mainly on the surface. The liquid part either evaporates or is absorbed by the coating layer. Uncoated papers show a different behaviour. Due to their relatively open surface structure, the pigments are able to enter the upper part of the surface and become less visible. For that reason, prints on uncoated papers look pale compared to similar prints on coated papers. Less ink is thus needed for coated than for uncoated substrates. In order to achieve this with the IGT-F1, a different anilox roll with

less ink transfer capacity was chosen for the prints on coated substrates. Furthermore, a lower contact pressure for the anilox and printing cylinder was set.

Table 5 *Paper grades used in full-scale printing*

Variable	Settings for uncoated qualities
IGT-F1	Printing force = 45 N
	Anilox force = 30 N
	Printing speed = 0.6 m/s
	Revolutions = 2
Anilox roll	Cell volume 2.7 ml/m²
	Angle 60°
	Resolution of 235 l/cm
	IGT-Ref.no.: 402.419
Printing cylinder	Cylinder-Ø 166 mm
	Tape 0.55 mm (DuploFLEX 5.3, Lohmann)
	DuPont DPC digital cliché t = 1.7 mm 40 Shore A
Ink	SunChemical, diluted with demineralized water and adjusted to 21 s with DIN Cup #4

Ink-jet printing

Ink-jet printing was chosen to be compared with flexo printing because this is a non-impact method (see chapter “Methods”). The print layout consisted of six cyan squares, one in the centre, one in each corner and the others in between. The squares were printed in fulltone areas in a size of 100 x 100 mm.

5.2 Results

Topography

As for the laboratory trials, the first step is the examination of the topography of the substrate. Stepwise the measurements reach the micro scale and the results become more precise. To obtain comparable results, the same measurement system with similar settings was used. In the case of CLSM an unpredicted problem appeared. The lower surface roughness on the peaks led to reflections during the measurements. These made the results in terms of surface roughness unusable.

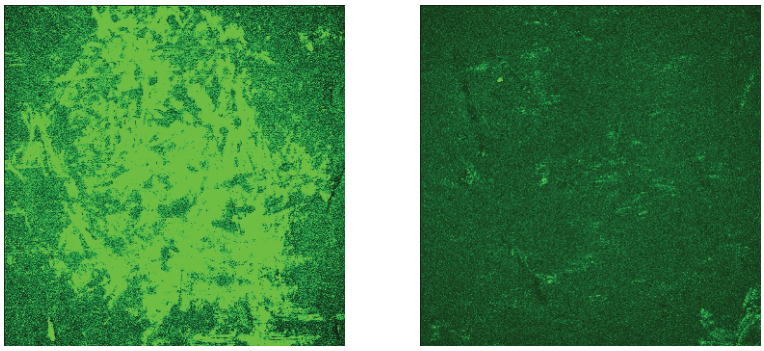

Figure 22 *CLSM images (10x magnification) taken from a glossy area (left) and in between in the valley (right).*

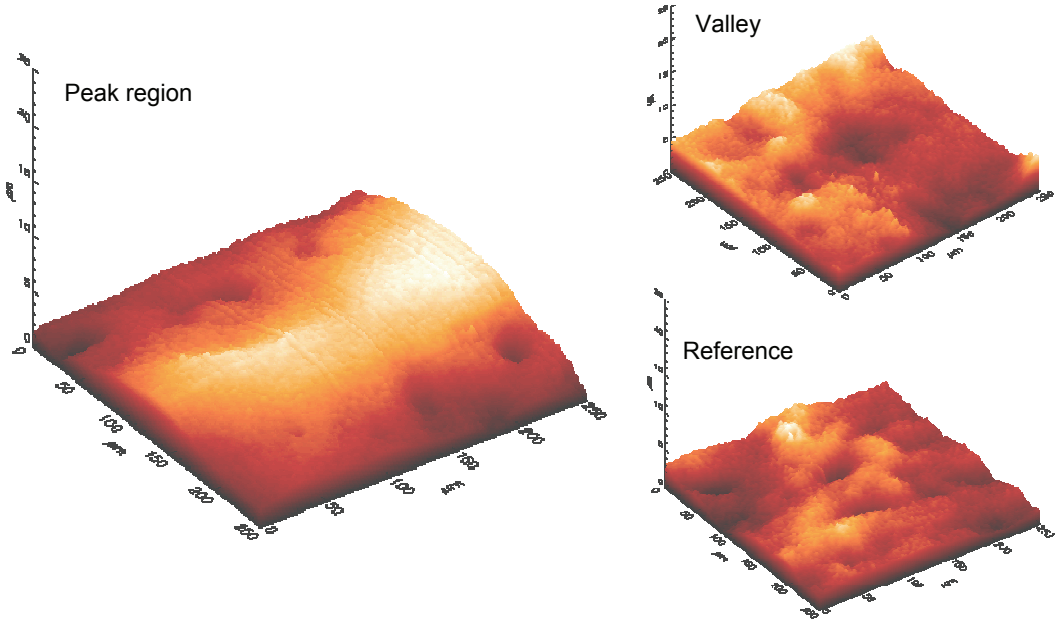

Figure 23 *FRT MicroProf images (250 x 250 µm, resolution of 1µm / pixel, 25 µm in z-direction); left: peak area, wavy structure of the liner is recognizable; top-right: valley area; bottom-right: reference.*

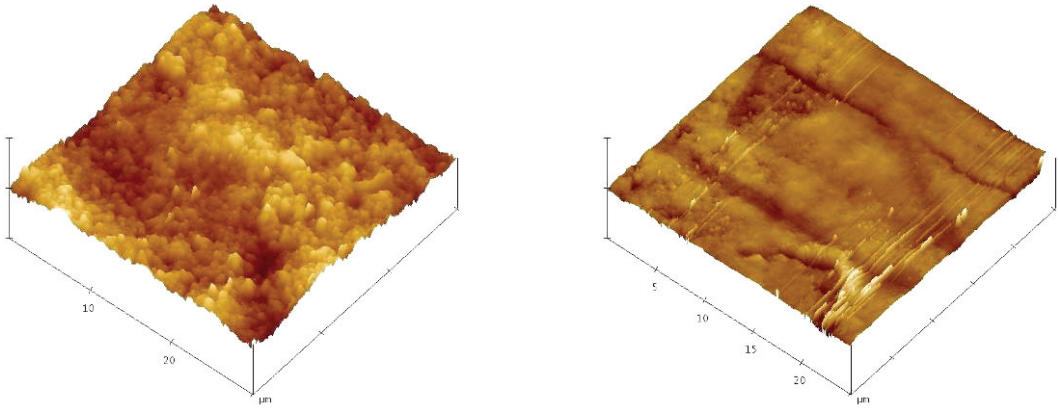

Figure 24 *AFM images; left: reference sample (30 x 30 µm, Rq= 139.76 nm), taken from the paper roll at the reel stand; right: treated sample (25 x 25 µm, Rq= 52.03 nm), peak-area on the liner; failures in the right hand image caused by problems during the measurements.*

However, it was possible to calculate an image from all taken layers. The glossy structure is clearly visible in the left-hand image in figure 22. Based on the gloss measurements, distributed later on in this chapter, sample S4c was used for all further measurements.

Pre-studies with FRT-MicroProf at an x-y resolution of 5 µm/pixel showed that too low resolution leads to incorrect results. This system measures in the micro-scale, but the surface roughness on coated papers appears on a nano-scale. Even the maximum lateral resolution of 1 µm/pixel was too low for exact values, but it should be enough for a good trend. In addition, the size of the measurement area is important, since there is a risk to measure not only the gloss region but to include some parts of the valley. Images with a larger image size were therefore captured to locate the peak areas. In the computer program, the larger image with the dimensions of 1 x 1 mm was cropped to smaller scan areas of 0.5 x 0.5 mm and 0.25 x 0.25 mm within the peak or valley areas. In figure 23 are illustrated images of a peak, valley and reference region within the smallest image size of 250 x 250 µm. A comparison of a series of different resolutions is included in the appendix.

AFM was chosen to replace CLSM from the laboratory test. Still some problems aroused when measuring glossy regions. Particles from the coating surface adhered to the measuring head and falsified the scan. This was mostly visible with at a larger measuring range, and partly it is shown in the right hand image of figure 24. This figure shows the difference between glossy area and untreated reference paper regarding topography on a nano-scale.

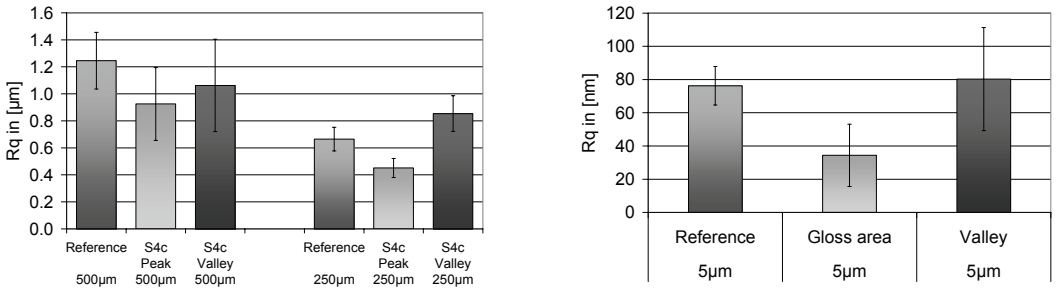

Figure 25 *FRT MicroProf (left) and AFM (right); the value below the sample indicates the length of the square measurement area.In both cases, the surface roughness is lower in the peak regions.*

A smaller metering range of 5 x 5 µm was chosen for the evaluations. This smaller range delivered reasonable results and these are shown in direct comparison with the FRT MicroProf results in figure 25. The two methods correlate with each other; the surface roughness on the peak or gloss area is less than that of the reference and the valley. Only the change between reference and valley was significantly different. This is partly due to the corrugated board

production process. Some spots in the valley were in contact with the heating plate in the double-backer and thus exposed to shear. This was leading to a high standard deviation of the MicroProf measurements. Anyhow, the important result is not the magnitude of difference in exact numbers. Instead, trends were detected. Differences in surface roughness between peak and valley could be detected. As cognizable in figure 25, this difference in surface roughness is high and it approves the visual judgement. The AFM images used for the evaluation can be found in the appendix.

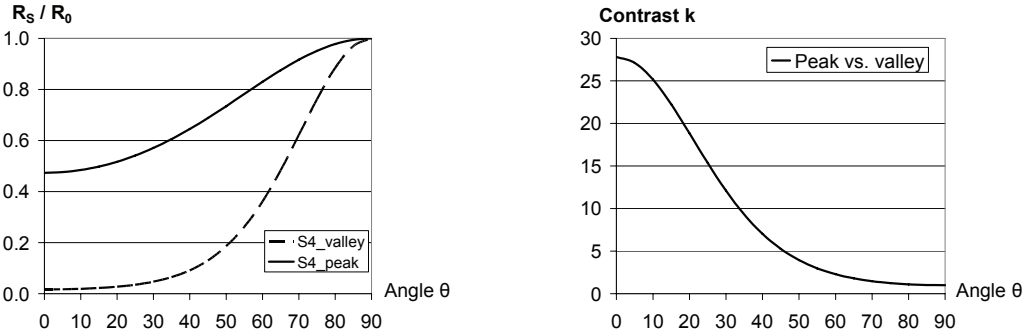

Figure 26 *Left: Roughness attenuation of the specular reflectance; the higher the value the higher the gloss appearance; right: Contrast k between peak and valley. The higher the value the higher is the contrast between gloss (peak) and non-gloss (valley) areas.*

The diagrams in figure 26 have been calculated using equations 2.3 and 2.4. The plot of R_s/R_0 against the incident angle θ_i shows high reflectance values for the peak and low values for the valley at a low incidence angle. The result is a high contrast between the two areas, as is shown in the right diagram. With increasing incidence angle (light beam becomes parallel to the paper surface), both peak and valley increase, but the valley values start to increase dramatically at 45°. Simultaneously the contrast k declines, meaning that the gloss difference decreases with increasing angle. At 90°, both areas have the same gloss appearance and no difference in gloss between peak and valley is visible.

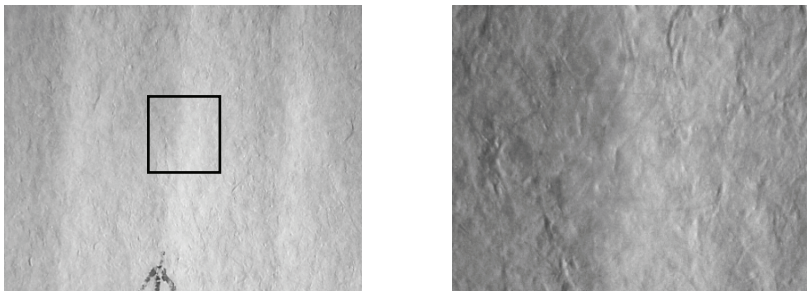

Figure 27 *Light Microscopy images with an illumination angle of 5° from the paper surface plane; left: the fibre structure can be observed, visible through the coating; right: illustrates a glossy area in the centre; the peak lines are aligned vertically.*

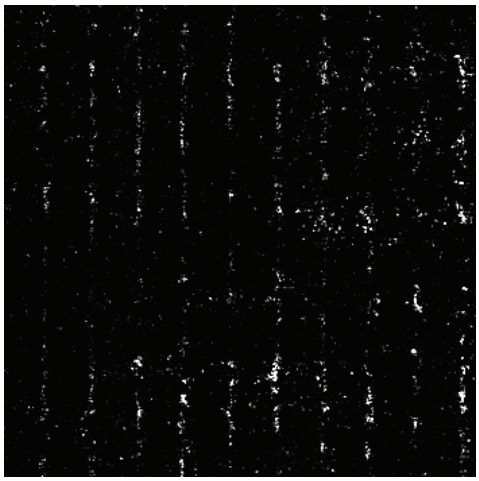

Figure 28 *Gloss image of the sample S4c; captured with STFI MicroGloss meter.*

The surface roughness change and gloss effect can be determined with the STFI MicroGloss meter. The image of sample S4c is shown in figure 28. This image shows the surface changes and how strongly these changes are perceivable. Images of other samples from the pilot trial are presented in the appendix. The glossy stripes are not uniform. The stripes are discontinuous and in some regions they appear thicker. This is presumably dependent on the substructure, the fluting of the corrugated board. Section-wise weakened fluting and differences in glue are two possible explanations. Furthermore, as shown in figure 27, the paper surface thus the paper thickness could be not uniform, too, and creating such irregular glossy stripes.

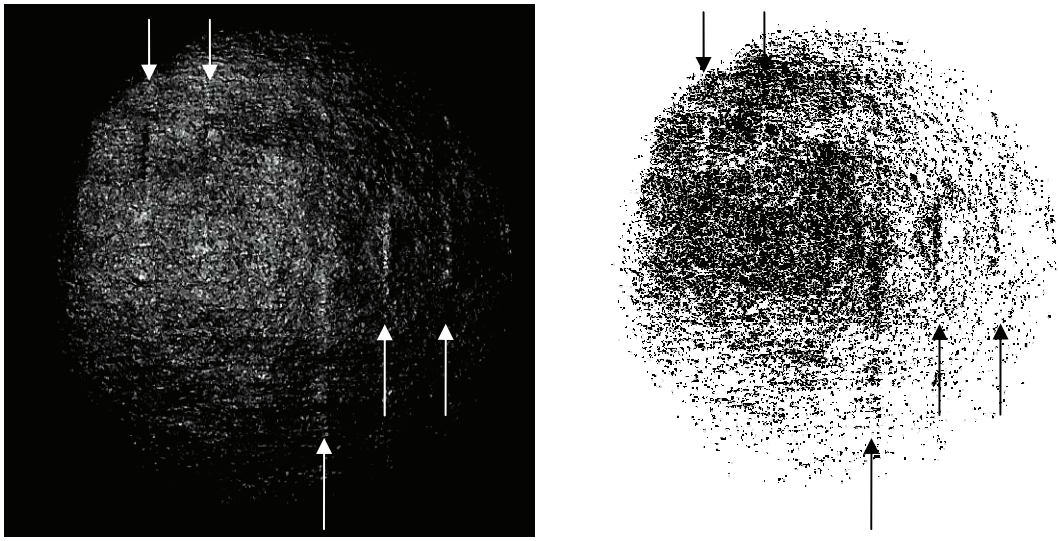

Figure 29 *Gloss image of the printed sample S4c; taken with provisional test set-up; the left image is the original and the right is a post-processed negative image of the original to emphasize the gloss areas; the arrows indicate the glossy lines/spots.*

Print analysis

As explained in Paper II and III, print analysis with gloss measurements was almost impossible. The gloss effects of the substrate were not detectable with the STFI MicroGloss. The micro-surface roughness was levelled out by the ink and the surface gloss was covered by the print gloss. However, gloss effects were visible to the eye and a provisional test was therefore conducted with 45° / 45° angles of incidence and reflection. In order to prevent the impression of washboarding by shading effects, the flute lines of the samples were set parallel to the light beam. The image, captured from sample S4c, is illustrated in figure 29. It includes two images, the original from the camera (left) and a post-processed negative image to highlight the glossy areas (right). In both images, the glossy lines/spots are distinguishable. Both images are illustrated to make it easier to recognize these glossy stripes/areas on the peak.

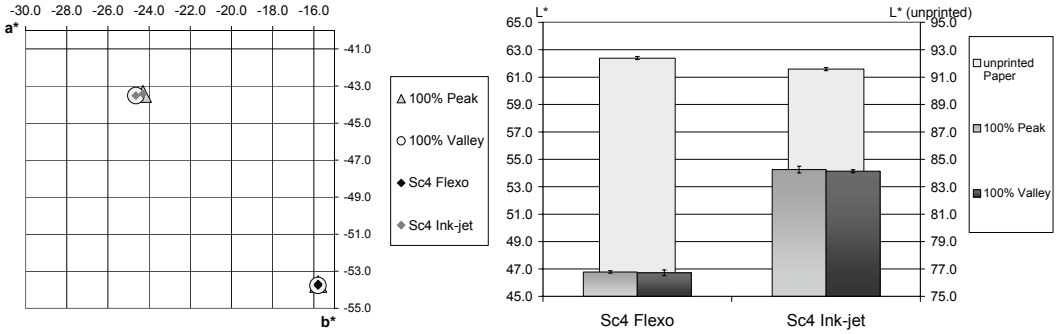

Figure 30 *Print analysis results; left: the a*b*-values of the sample S4c measured on the peak and in the valley and both in the fulltone area; right: L*-values, the front bars belong to the left primary axis and the chart behind belongs to the right secondary axis.*

The colour was measured with the Spectrodensitometer with the same settings on the measurement system as in the laboratory test. The left chart in figure 30 is illustrating the values of the sample S4c in the a*b* coordinate system. No shift is visible between peak and valley. Only the divergence between the two printing methods, flexo and ink-jet print, can be seen. Similar result is given by the L* values in the right diagram. The colour difference ΔE in figure 31 displays a similar result; the difference is insignificant. All three charts are telling that not even a slight shift in colour is detectable between peak and valley. The print appears to be completely uniform.

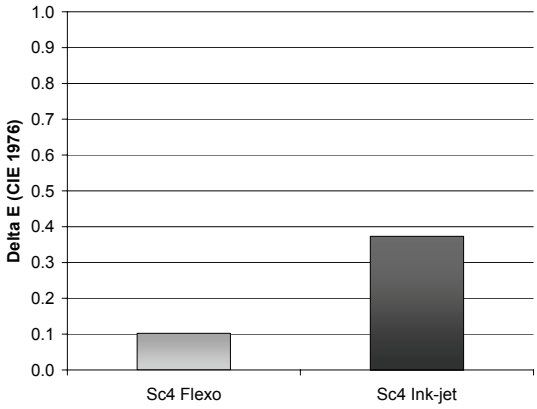

Figure 31 *ΔE between peak and valley measurements in the a*b* colour diagram.*

5.3 Discussion

To summarize the knowledge gained from this pilot trial, surface roughness changes on a micro scale occur on the liner during the production of corrugated board. As the STFI MicroGloss measurements revealed, the uncoated samples did not show any gloss effect in the unprinted state. Therefore, this series was excluded from further evaluation. The reasons behind are yet unexplored and it could be, that the type and age of the corrugator might have a further influencing factor.

The coated samples, however, showed a very clear result. The gloss appearance is visible with the eye and can be measured with the STFI MicroGloss meter. This was checked and supported by all surface roughness measurement. These were performed on macro-, micro- and nano-scales, all with the same result. The surface roughness along the peaks was lower than that of the reference and the valleys. Therefore can be concluded, the coating layer is less resistant to heat, pressure and friction. The magnitude of the affected areas is then dependent on the corrugator settings. The highest influence was generated by slowing down the corrugator. The samples with increased temperature in the pre-heater and double-backer show very little influence compared to the sample chosen as reference (Sc1).

The colour data were not as useful as expected. The L*a*b* colour measurements are surprisingly little influenced and even negligible, considering the results gathered in the topographical measurements. A possible explanation could be that the effects described in this thesis affect only the gloss appearance but not the colour.

6 Conclusion

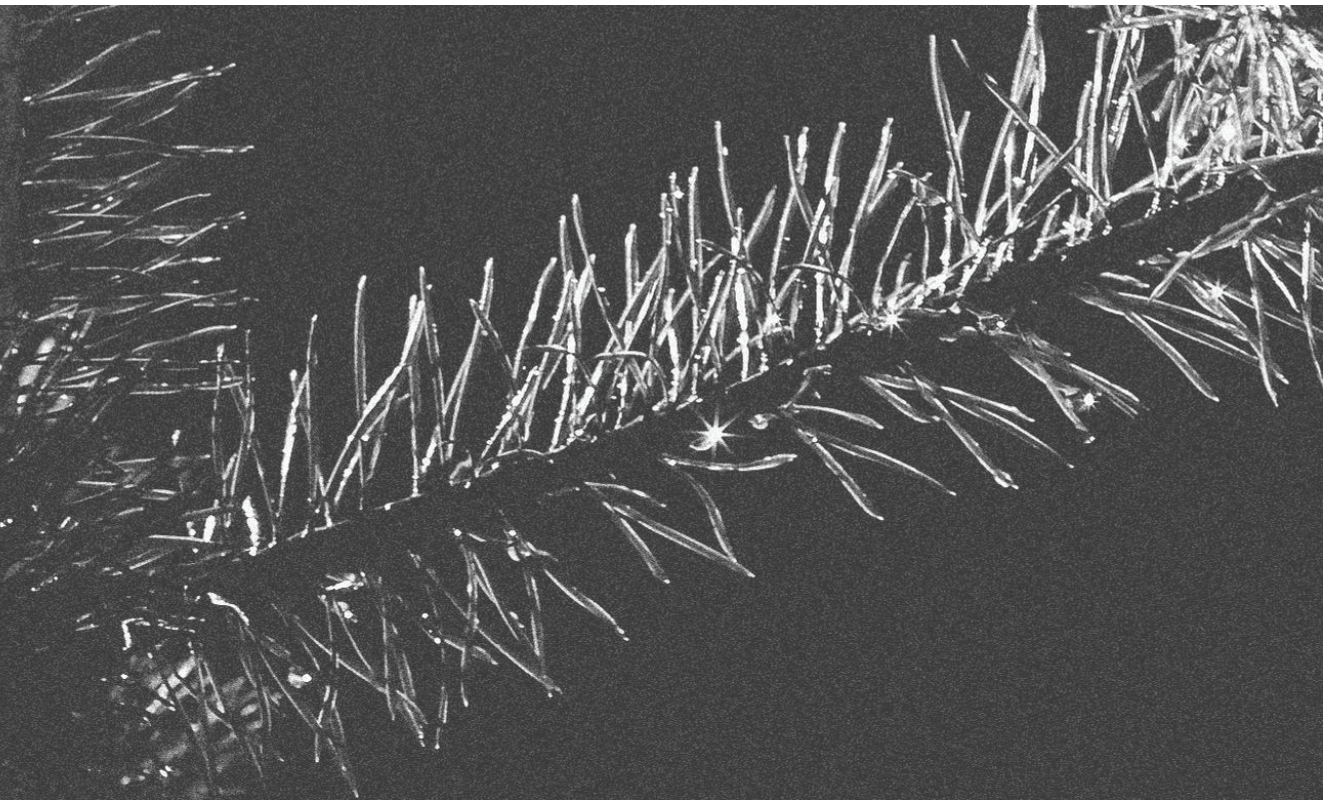

6.1 Summary

Trials in the laboratory and on a full scale have been performed to state topographical effects on corrugated board liner during the production in the corrugator. The micro-scale changes in surface roughness were examined by a pivotal study. In both trials it was possible to show evidence of the existence of surface impacts by the corrugated board production process. For the laboratory tests, the uncoated grades and for the pilot trials the coated grades were evaluated. In both cases, the counterpart was excluded from the evaluation due to the lack of reliable results. The evaluated samples showed conclusive results. The surface roughness in the peak area was decreased in relation to the untreated reference and the valley area. Measuring with higher resolution and smaller measurement area delivered more constant and accurate values; the AFM system enabled this.

Concerning the print analysis results, the samples prepared in the laboratory showed colour and print density shifts. For the fulltone area only to a minor degree, but the 70% halftone area lets assume that the ink film thickness is increased on the peak compared to the valley. It was not possible to say whether this was due to surface roughness changes or to the washboarding effect. In the case of the coated samples in the full-scale test, no effect at all was detectable. A reason could be that the ink is capable of forming an ink film layer on top of the surface of the paper. This would cover the micro roughness of the matt parts creating an almost homogeneous glossy appearance.

The process step responsible for these changes in paper surface should be located in the corrugated board production process. The most probable process step is the double-backer. Therefore, counteractive measures should be discussed. Johansson et al. (1991, 1995) state that friction is an important parameter affecting the paper surface. Back (1991) mentioned that a low coefficient of friction of paper against metal is desirable in the corrugator, i.e. that highly polished metal surfaces are important. Changes in the design of the hot plates in the double-backer can contribute to a lower friction coefficient and so to minimize the wear effect.

In that respect the result agree with the study performed by Odeberg Glasenapp (2004). The existence of surface roughness differences on a micro-scale between peaks and valleys is confirmed by several measurement methods. In both trials, even with different types of substrates (coated and uncoated), the same trend was detected, but the print result was affected less than expected.

6.2 Recommendation for future work

The laboratory test has provided a good opportunity to produce first results with greater latitude. In comparison with the full-scale test, the lab-test has to be improved. More focus should be given to different types of substrates and coatings. Some may be affected to a greater extent and others less. A condensed but relevant version of topographical tests should be performed, including AFM and for validation the FRT MicroProf. In the case of gloss, the measurements failed for the printed coated samples in the STFI MicroGloss meter and a provisional measurement system was used. More study on this could be useful, as well as on finding another method to reveal gloss effects between peak and valley regions. Adjustments in the printing process, like less ink application, could give rise to gloss effects in print and make it easier to evaluate.

References

Back, E. L. (1991)
Paper-to-paper and paper-to-metal friction. In 1991 International Paper Physics Conference. Kona, Hawaii. TAPPI Press, p. 49-65.

Barros, G. G. (2006):
Influence of substrate Topography on ink distribution in flexography. Dissertation. Karlstad University, Karlstad, Sweden. ISBN: 91-7063-048-8.

Béland, M.-C., Lindberg, S. and Johansson, P.-Å. (2000):
Optical measurement and perception of gloss quality of printed matte-coated paper. Journal of Pulp and Paper Science, Vol. 26, No. 3, p. 120-123.

Bennett, J. M. and Mattsson, L. (1999):
Introduction to surface roughness and scattering. 2nd ed. Washington DC: Optical society of America. ISBN: 1-55752-609-5.

Brehm, P. V. (1992):
Introduction to Densitometry. 3rd ed. Alexandria, USA: Graphic Communications Association. ISBN: 0-933505-10-8.

Chalmers, I. R. (1998):
Flexographic printability of packaging grade papers. Appita Journal, Vol. 51, No. 3, p. 193-198. ISSN: 1038-6807.

Cusdin, G. B. (2000):
Why does 'washboard' show up in my print? Flexo, Vol. 25, No. 1, p. 28-30, 32, 34, 36.

Hallberg Hofstrand, E. (2006):
Flexographic post-printing of corrugated board. Dissertation. Karlstad University, Karlstad, Sweden. ISBN: 1403-8099.

Hering, E., Martin, R. and Stohrer, M. (1999):
Physik für Ingenieure. 7th Edition ed. Heidelberg: Springer-Verlag.

Holmvall, M. (2007):
Striping on Flexo Post-Printed Corrugated Board. Licentiate Thesis. Mittuniversitetet - Mid Sweden University, Sundsvall, Sweden. ISBN: 978-91-85317-63-9.

IRI (2006):
Der Shopper 2006 am POS. IRI Information Resources GmbH
Pro Carton Deutschland, Nürnberg. http://www.procarton.de/iri.php (2007-09-24).

Johansson, A., Fellers, C., Gunderson, D. and Haugen, U. (1991):
Paper friction - influence of measurement conditions. Tappi Journal, Vol. 81, No. 5, p. 175-183.

Johansson, A., Fellers, C., Gunderson, D. and Haugen, U. (1995)
Paper Friction - Influence of Measurement Conditions. In 1995 International Paper Physics Conference. Niagara-on-the-Lake, Canada. TAPPI Press, p. P5 - P15. ISBN: 1-895288-87-8.

Johansson, P.-Å. (1999):
Optical homogeneity of prints. Doctoral Thesis. KTH - Royal Institute of Technology, Stockholm, Sweden. ISSN: 1104-7003.

Johansson, P.-Å. and Christiansson, H. (2004):
MicroGloss by STFI-Packforsk - a way of measuring gloss quality as we percieve. STFI-Packforsk, Stockholm. http://www.stfi.se/upload/2218/MicroGloss.pdf (2007-10-09).

Kipphan, H. (2001):
Handbook of Print Media. Heidelberg, Germany: Heidelberger Druckmaschinen AG. ISBN: 3-540-67326.

Lindberg, S. (2004):
Perceptual determinants of print quality. Doctoral Thesis. Stockholm University, Stockholm. ISBN: 91-7265-905-X.

Lindstrand, M. (2002):
Gloss: measurement, characterization and visualization-in the light of visual evaluation. Licentiate Thesis. Linköpings Universitet, Campus Norrköping, Stockholm. ISBN: 91-7373-451-9.

Louman, H. W. (1983):
Relation zwischen Oberflächenreflexion und Druckglätte. Wochenblatt der Papierfabrik, Vol. 111, No. 14, p. 496-500.

Mensing, H. (2006):
Private communication. BHS-Corrugated, Weiherhammer, Germany. March 2006.

Meyer, K. H. (1999):
Technik des Flexodrucks. Germany: Deutschsprachige Flexodruckfachgruppe e.V. (DFTA). ISBN: 3-85599-003-4.

Moss, E. A., Relulainer, E., Paulapuro, H. and Aaltonen, P. (1993):
Taking a new look at pulp and paper: Applications of confocal laser scanning microscopy (CLSM) to pulp and paper research. Paperi ja puu - Paper and Timer, Vol. 75, No. 1-2, p. 74-79.

Netz, E. (1996):
Washboarding and print quality of corrugated board. Licentiate Thesis. KTH - Royal Institute of Technology, Stockholm. ISBN: ISSN 1104-7003.

Odeberg Glasenapp, A. (2004):
A journey in the micro structure of flexo printed corrugated board. STFI-Packforsk AB, Stockholm, Sweden. p. 15, http://www.t2f.nu/t2frapp_f_122.pdf, March 2004.

Odeberg Glasenapp, A. (2004)
Flexo post-printing of corrugated board - Attempts to explain stripiness. In 14th IAPRI World Conference on Packaging. Stockholm, Sweden.

Pauler, N. (2002):
Paper Optics. Kista, Sweden: AB Lorentzen & Wettre. ISBN: 91-971765-6-7.

Pedraza, R. (1993):
Eliminating Washboard Worries. Boxboard Containers, Vol. 100, No. 8, p. 36-38.

Persson, B. N. J. (2000):
Sliding Friction - Physical Principles and Application, ed. Von Klitzing, K. and R. Wiesendanger. Heidelberg: Springer-Verlag. ISBN: 3-540-63296-4.

Pinnington, T. (2003):
Wet End - Combining. In The corrugated industry - In pursuit of excellence, Brunton, M., Editor. Brunton Technical Publications Ltd, p. 87-93.

Rehberger, M. (2004):
Print Quality of flexographic printed Corrugated Board. Diploma Thesis. University of Applied Sciences, Regensburg, Germany.

VDW (2006):
Wellpappe macht es möglich: Mit multisensorischem Marketing die Sinne ansprechen. VDW - Verband der Wellpappen-Industrie e.V., Darmstadt. http://www.resy-gmbh.online.de/ps/ps_wr_306a.htm (2007-09-24).

Zang, Y. H. and Aspler, J. S. (1995):
Factors that affect the flexographic printability of linerboards. Tappi Journal, Vol. 78, No. 10, p. 240-23 - 240-33.

Appendix

FRT MicroProf images – Pilot Trial, unprinted sample Sc4

Reference

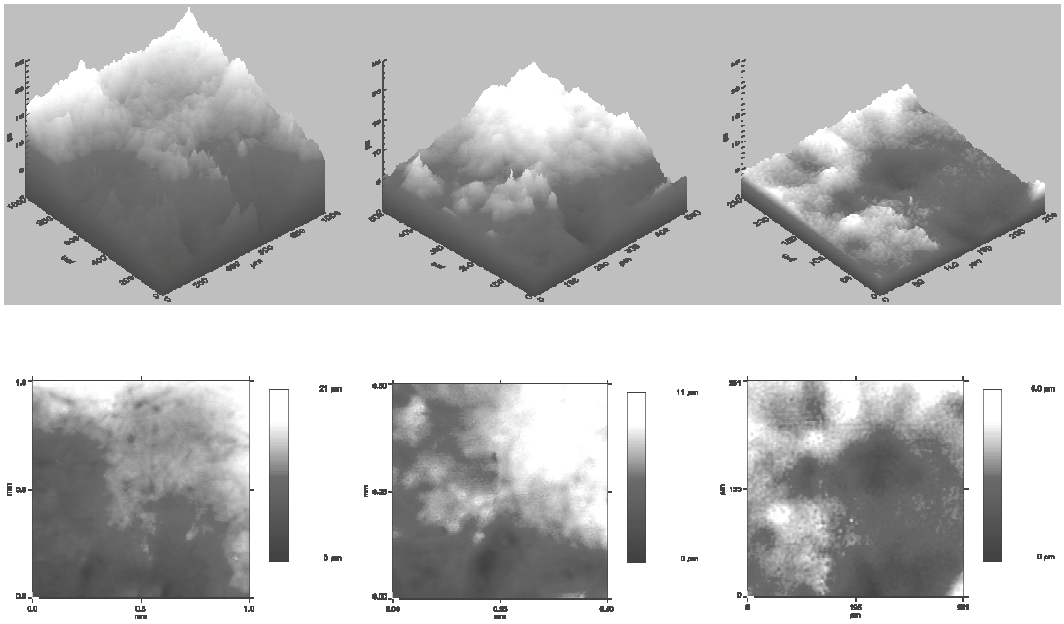

Figure 32 *Reference images in 3D (top) and 2D (Bottom) resolution of 1µm / pixel, 25 µm in z-direction: left: 1000 x 1000 µm; middle: 500 x 500 µm; right: 250 x 250 µm*

Flute-peak

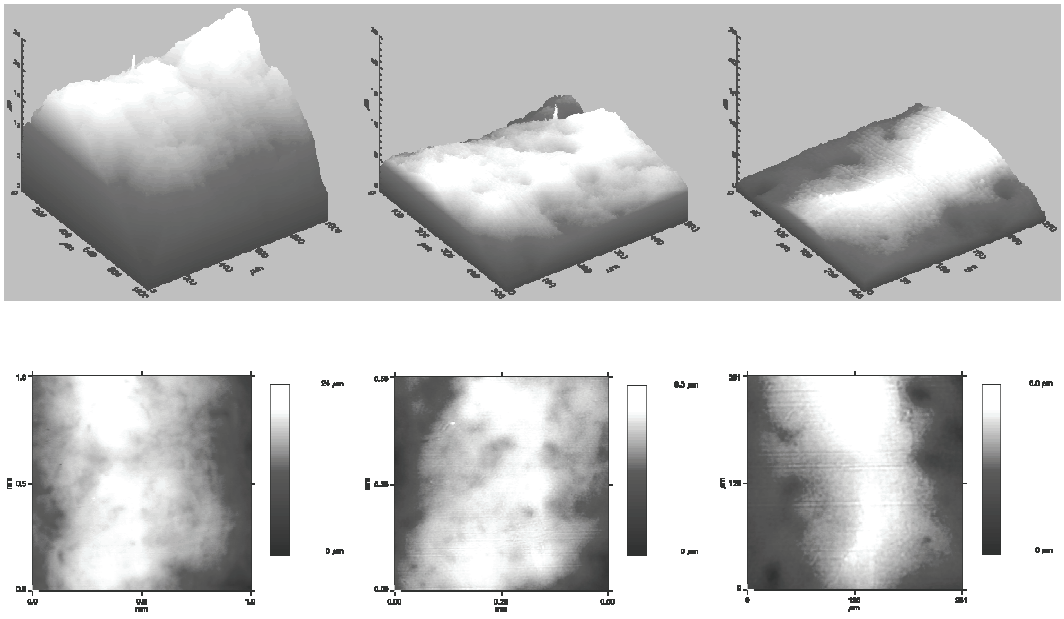

Figure 33 *Peak images in 3D (top) and 2D (Bottom) resolution of 1µm / pixel, 25 µm in z-direction: left: 1000 x 1000 µm; middle: 500 x 500 µm; right: 250 x 250 µm*

Valley

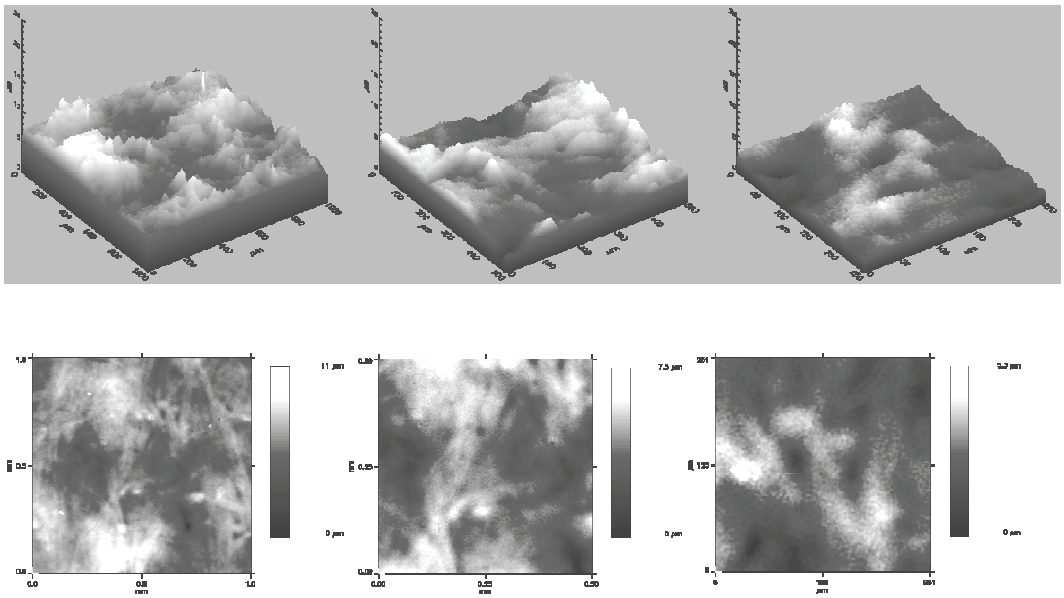

Figure 34 *Valley images in 3D (top) and 2D (Bottom) resolution of 1µm / pixel, 25 µm in z-direction: left: 1000 x 1000 µm; middle: 500 x 500 µm; right: 250 x 250 µm*

AFM-images – Pilot Trial, unprinted sample Sc4

Reference (5 x 5 µm)

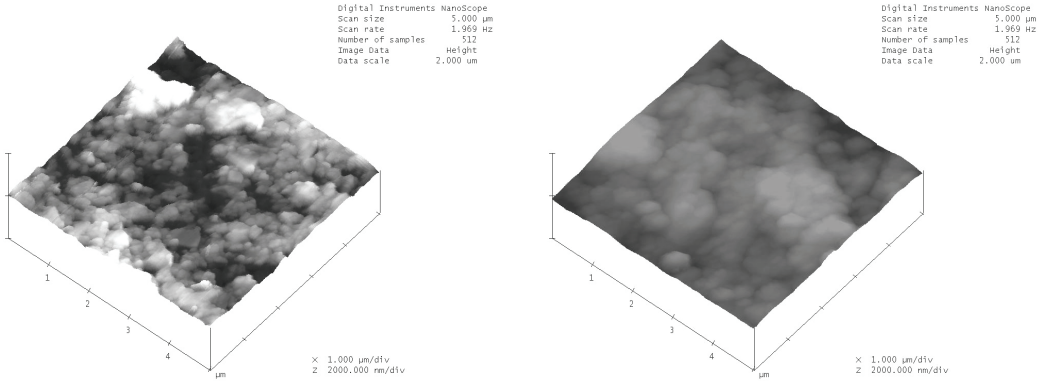

Figure 35 *Left: Reference 1 (Rq= 84.48 nm); right: Reference 2 (Rq= 68.03 nm); taken sample from the liner roll at the reel stand.*

Flute-peak (5 x 5 µm)

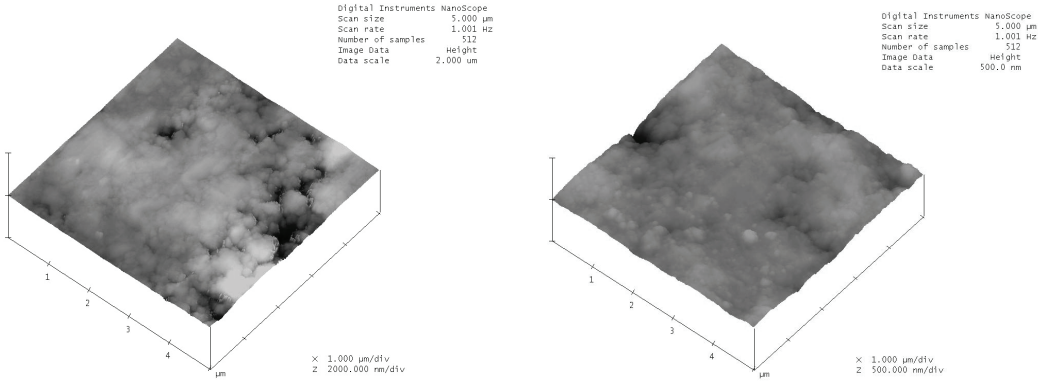

Figure 36 *Left: Peak 1 (Rq= 29.16 nm); right: Peak 2 (Rq= 18.76 nm); Glossy area on the flute peak.*

Valley (5 x 5 µm)

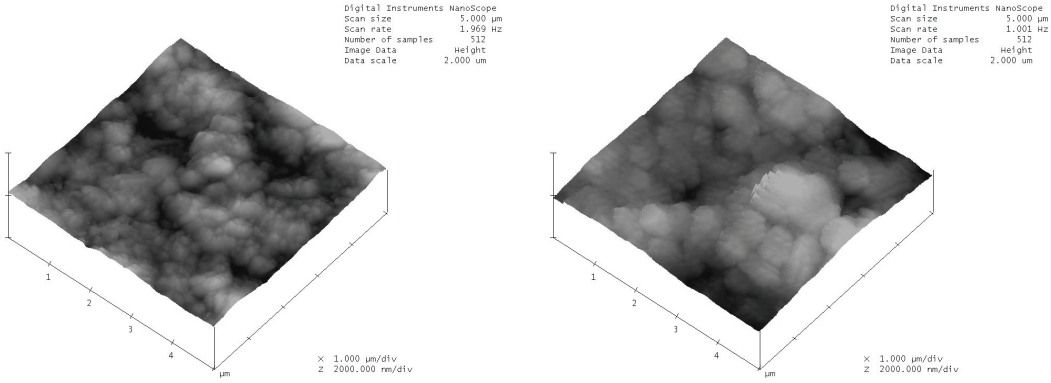

Figure 37 *Left: Valley 1 (Rq= 102.20 nm); right: Valley 2 (Rq= 58.30 nm);Area between to flute peaks.*

MicroGloss – Pilot Trial, unprinted samples

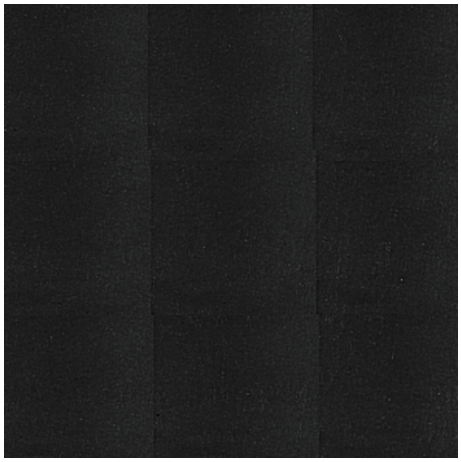

Figure 38 *uncoated sample Su1*

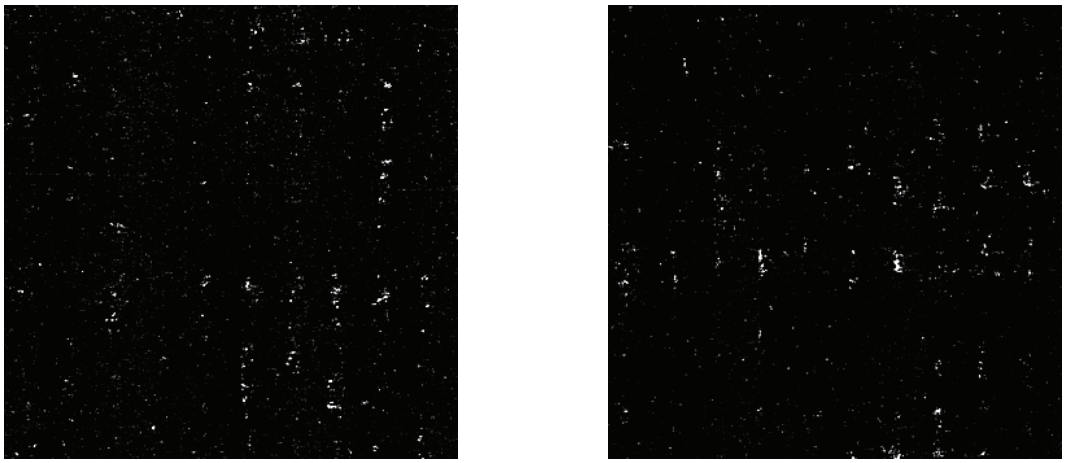

Figure 39 *coated samples Sc1 (left) and Sc2 (right)*

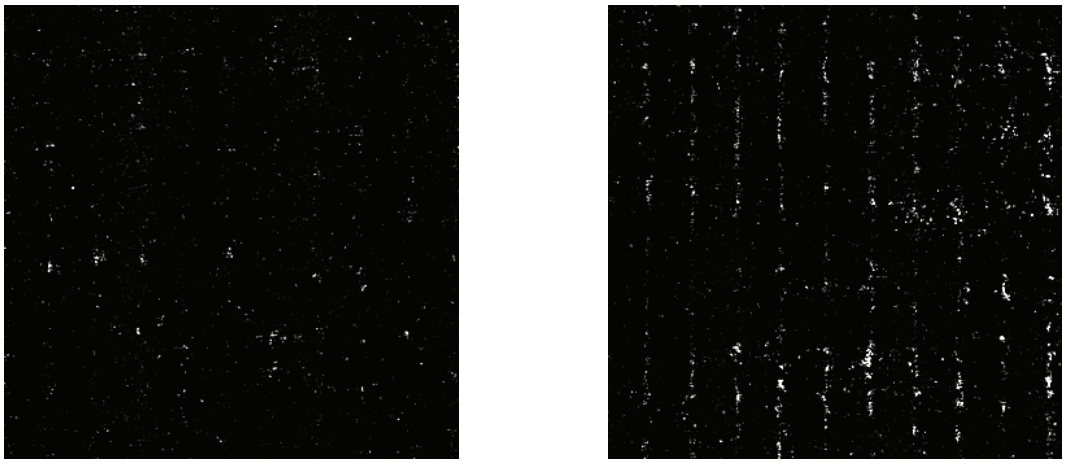

Figure 40 *coated samples Sc3 (left) and Sc4 (right)*

L a b* - Results of laboratory trial and full-scale test*

Table 6 *L*a*b* data for samples of laboratory trial*

L* a* b*		1u110_10sM Average	Std. Dev.	1u170_10sM Average	Std. Dev.	2u100_10sM Average	Std. Dev.	2u175_10sM Average	Std. Dev.	2u100_10s Average	Std. Dev.	2u175_10s Average	Std. Dev.
L*	unprinted Paper	90.134	0.265	90.796	1.083	91.478	1.131	92.149	0.141	91.487	0.970	90.924	0.864
	100% REF	48.868	0.421	49.406	0.742	49.738	0.792	50.166	0.181	49.933	0.293	49.963	0.377
	100% Peak	48.660	0.251	49.033	0.556	49.257	0.491	49.513	0.248	49.323	0.232	49.422	0.313
	100% Valley	48.854	0.287	49.174	0.606	49.373	0.606	49.874	0.386	49.796	0.441	49.904	0.455
	70% REF	57.771	0.415	57.911	0.390	57.991	0.335	58.104	0.298	58.102	0.262	58.027	0.298
	70% Peak	55.138	0.682	55.626	0.562	55.666	0.581	55.894	0.566	55.636	0.580	55.317	0.636
	70% Valley	58.244	0.459	58.688	0.922	58.817	0.866	59.257	0.613	58.850	0.488	58.859	0.575
a*	unprinted Paper	0.907	0.095	0.686	0.322	0.480	0.272	0.316	0.054	0.311	0.066	0.293	0.072
	100% REF	-10.914	0.405	-11.319	0.608	-11.670	0.698	-12.074	0.241	-11.870	0.438	-11.572	0.398
	100% Peak	-10.422	0.303	-10.688	0.361	-10.784	0.366	-10.997	0.393	-10.822	0.467	-10.747	0.527
	100% Valley	-11.126	0.198	-11.501	0.642	-11.703	0.684	-12.214	0.491	-11.940	0.586	-11.821	0.546
	70% REF	-9.864	0.146	-10.240	0.599	-10.672	0.650	-11.116	0.167	-10.667	0.764	-10.162	0.768
	70% Peak	-10.063	0.295	-10.548	0.865	-11.026	0.816	-11.428	0.264	-10.874	0.661	-10.424	0.569
	70% Valley	-9.727	0.184	-10.161	0.648	-10.609	0.626	-11.027	0.173	-10.593	0.706	-10.182	0.679
b*	unprinted Paper	0.910	0.104	0.912	0.095	0.942	0.113	0.987	0.055	1.273	0.434	1.491	0.420
	100% REF	-44.411	0.299	-44.587	0.508	-44.950	0.452	-45.223	0.069	-44.670	0.838	-44.032	0.896
	100% Peak	-44.202	0.255	-44.469	0.385	-44.863	0.382	-45.104	0.290	-44.649	0.886	-44.012	0.955
	100% Valley	-44.429	0.379	-44.803	0.450	-45.234	0.516	-45.369	0.399	-44.622	1.268	-43.879	1.003
	70% REF	-34.788	0.532	-35.303	1.093	-35.946	0.863	-36.404	0.477	-35.627	1.135	-34.891	1.163
	70% Peak	-37.347	0.666	-37.677	1.155	-38.320	1.105	-38.690	0.755	-38.192	0.757	-37.626	0.669
	70% Valley	-34.151	0.551	-34.409	0.579	-34.937	0.661	-35.126	0.608	-34.642	1.213	-34.011	1.001

Table 7 *L*a*b* data for samples of full-scale test*

L* a* b*		Sc4 Flexo Average	Std. Dev.	Sc4 Ink-jet Average	Std. Dev.
L*	unprinted Paper	92.392	0.118	91.586	0.120
	100% Peak	46.784	0.086	54.256	0.244
	100% Valley	46.719	0.215	54.134	0.107
a*	unprinted Paper	1.096	0.072	1.212	0.185
	100% Peak	-15.787	0.172	-24.300	0.142
	100% Valley	-15.798	0.223	-24.642	0.154
b*	unprinted Paper	-3.602	0.262	-3.334	0.348
	100% Peak	-53.687	0.225	-43.428	0.191
	100% Valley	-53.765	0.120	-43.514	0.195

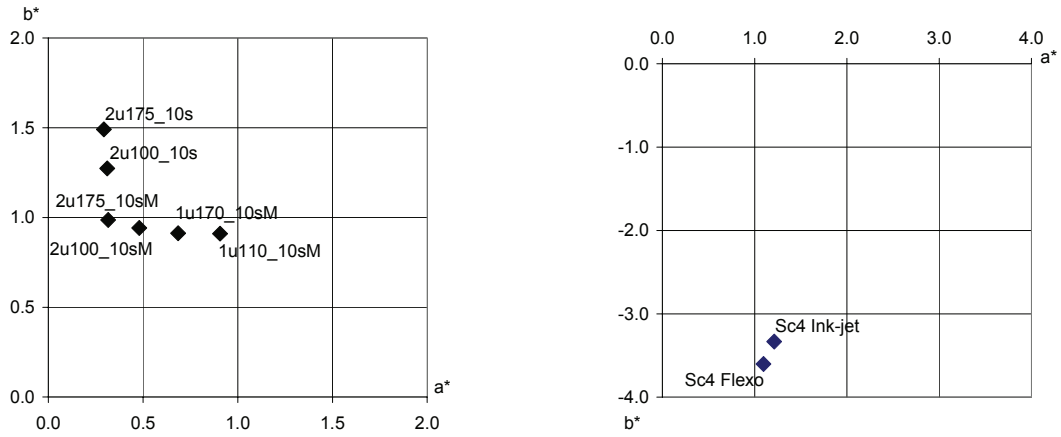

Figure 41 *L* values of the unprinted part of each sample; left: laboratory trial; right: full scale test; index flexo means flexographic printed sample S4c and respectively ink-jet printed*

MicroGloss – Pilot Trial, printed samples

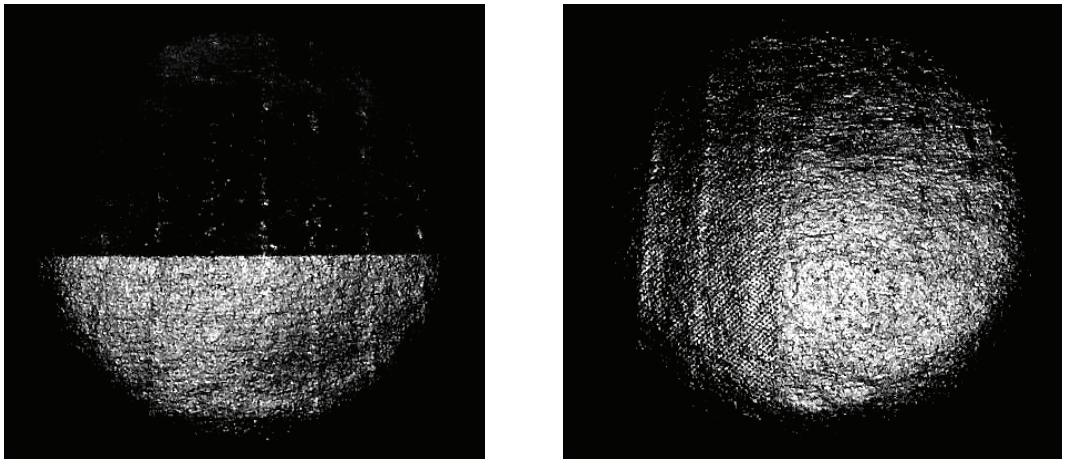

Figure 42 *Gloss image of the sample S4c; taken with provisional test set-up; left: the transition between unprinted (top) and ink-jet (bottom) printed part of sample S4c; right: flexo printed sample S4c with halftone (left) and fulltone (right).*

The authors' contribution to the papers

Paper I

Rehberger, M., Odeberg Glasenapp, A., Johansson, P.-Å., Gällstedt, M.
Topographical micro changes of corrugated board liners induced by heat treatment and their effect on flexographic print quality.
I have carried out the research in the study. Astrid Odeberg Glasenapp developed the initial idea. I planned the trials, did all the measurements and analyzed together with Per-Åke Johansson the results. Astrid Odeberg Glasenapp, Per-Åke Johansson and Mikael Gällstedt did the proofreading of this paper. I was responsible for the presentation of the paper.

Paper II

Rehberger, M., Odeberg Glasenapp, A., Johansson, P.-Å.
Topographical micro-changes on corrugated board liners – A comparison between laboratory and full-scale effects.
I have carried out the research in the study. I planned the trials, did all the measurements and analyzed together with Per-Åke Johansson the results. Astrid Odeberg Glasenapp and Per-Åke Johansson did the proofreading of this paper. I was responsible for the presentation of the paper.

Paper III

Rehberger, M., Odeberg Glasenapp, A., Johansson, P.-Å.
Corrugated board production and its micro-scale impacts on the liner's topography
I have carried out the research in the study. I planned the trials, did all the measurements and analyzed together with Per-Åke Johansson the results. Astrid Odeberg Glasenapp and Per-Åke Johansson did the proofreading of the paper. I was responsible for the presentation of the paper.